GIS-Based Statistical Landslide Susceptibility Modeling for Hazard Mitigation Planning in the Mai-Khola Watershed, Nepal Himalaya

Abstract

Landslides in Nepal's mid-hills represent a recurrent and devastating natural hazard, threatening lives, infrastructure, and agricultural land. This study aims to produce a robust landslide susceptibility zonation (LSZ) map for the landslide-prone Mai Khola watershed in Ilam District, Nepal, by applying Frequency Ratio (FR) and Weight of Evidence (WoE), within a Geographic Information System GIS-based comparative approach. A comprehensive, multi-temporal landslide inventory of 300 historical events was compiled from satellite imagery and field surveys to serve as the dependent variable. Eleven conditioning factors influencing slope stability elevation, slope angle, aspect, curvature, Topographic Wetness Index (TWI), geology, soil type, Normalized Difference Vegetation Index (NDVI), mean annual rainfall, and proximity to roads and rivers were derived from ASTER DEM (30 m resolution), Landsat imagery processed in Google Earth Engine, and Department of Hydrology and Meteorology (DHM) rainfall data (2001–2024).

The landslide inventory data were randomly divided, with 80% used for training the models and 20% reserved for validation. The resulting susceptibility maps were categorized into five hazard levels using the natural breaks method. Both models performed robustly, as confirmed by ROC curve analysis, though the Weight of Evidence (WoE) model demonstrated superior predictive accuracy (AUC = 0.866) compared to the Frequency Ratio (FR) model (AUC = 0.854), and provided a sharper spatial definition of high-risk areas. The WoE model also classified a larger portion of the watershed (24.64%) as High/Very High susceptibility compared to the FR model (14.40%). The analysis identified geology, NDVI, slope angle, and soil type as the most significant causative factors, with high-risk hotspots consistently located along steep valley slopes, river corridors, and near roads.

Keywords: Landslide Susceptibility Zonation (LSZ); Geographic Information System (GIS); Frequency Ratio (FR); Weight of Evidence (WoE); Statistical Modeling; Hazard Mapping.

This page is intentionally left blank

List of Figures

List of Tables

List of Abbreviations and Acronyms

DEM: Digital Elevation Model

GIS: Geographic Information System

AUC: Area Under Curve

ROC: Receiver Operating

TN: True Negative

TP: True Positive

FN: False Negative

FP: False Positive

FR: Frequency Ratio

WoE: Weight of Evidence

LSM: Landslide Susceptibility Mapping

NDVI: Normalized Difference Vegetative Index

DHM: Department of Hydrology and Meteorology

GEE: Google Earth Engine

TWI: Topographic Wetness Index

SN: Serial Number

FOS: Factor of Safety

LCF: Landslide Conditioning Factor

DMG: Department of Mines and Geology

Table of Contents

This page is left intentionally blank……..

Chapter 1 : Introduction

1.1 Background

Natural disasters like landslides are the most common hazards, especially in the hilly terrain characterized by steep slopes, weak, fragile geological structures, and tectonically active zones. Landslides involve the movement of materials (debris, rocks, soil, and earth) down the slope under the influence of gravity (Cruden, 1993a). They can be initiated by factors such as gravity, rainfall, earthquakes, and human activities like mining and construction. The ongoing challenges of climate change, heavy rainfall, seismic activity, and human activities collectively raise concerns about an increased incidence of landslides worldwide. Landslides rank as the third deadliest natural disaster globally, accounting for 9 % of global natural disasters.

Nepal, being located along the boundary of the Indian and Eurasian tectonic plates, is seismically active and highly susceptible to earthquakes and related natural disasters like landslides or slope failures (Bilham, 2019; Okamura et al., 2015a). The 2015 Gorkha earthquake tragically highlighted this seismic vulnerability, resulting in nearly 20,000 landslides. As per the Nepal Disaster Report 2019, over the past 49 years (from 1971 to 2019), Nepal has encountered approximately 3729 landslides that have led to loss of lives, displacement, and infrastructure damage. Out of all landslide occurrences recorded in the Global Fatal Landslide Database in the period between 2004 to 2016, 10 % occurred in Nepal (Froude & Petley, 2018a). Nepal's diverse geology, monsoons, and steep terrain result in devastating landslides, with over 90% occurring during the monsoon, peaking during July and August (Adhikari & Gautam, 2022). The number of landslides in Nepal has been dramatically increasing, particularly landslide concentrating along the mid-hill regions. Out of the 77 districts in Nepal, 49 districts, including Ilam, are prone to floods and/or landslides (Paudyal et al., 2013).

The main hazards that are repeatedly occurring and have a significant impact on lives and properties in Nepal are floods, landslides, debris flow, river channel shifting, avalanches, droughts, earthquakes, and epidemics. The occurrence of natural hazards is a serious constraint on economic development, particularly in developing countries, where the economic loss due to the impact of natural hazards often makes the difference between economic growth and stagnation. On average,

natural disasters take around 951 lives and damage property worth NRs 1,242 million every year in Nepal (DHM). Among these hazards, the overall impact caused by water-induced hazards floods, landslides, avalanches, riverbank cutting, and river shifting, is extremely high as compared to the loss due to other hazards.

Landslide assessment and mapping are crucial aspects of geo-hazard engineering and disaster management. Landslide assessment involves identification, categorization, and analysis of landslides in a specific area to assess their potential impact and mitigate risks. Analysis of landslide hazard is required to assess land damage, land depreciation, and sedimentation problems, which affect hydro-electric dams, flood control structures, bridges, roads, and irrigation channels. Landslide susceptibility assessment involves evaluating the probability of a future landslide occurrence in a specific geographical area, thereby predicting its potential locations (Guzzetti et al., 2005). Such a study helps to identify potential hazardous zones, assess the level of risk, and develop strategies to mitigate those risks (Dai et al., 2002a).

Several qualitative and quantitative approaches are available for the assessment and mapping of landslide susceptibility. Qualitative methodologies like the Heuristic approach and Multi-criteria decision analysis rely on expert judgments for spatial decision-making, while quantitative methods like Frequency ratio, and Weight of evidence methods involve assessing the probabilities associated with landslide events (Shano et al., 2020). Quantitative methods entail a numerical evaluation of the relationship between controlling variables (landslide factors) and past events (Baral et al., 2021a; Sarkar & Kanungo, 2006; Wang et al., 2021)). The combination of the World Web, satellite images, Geographical Information System (GIS), public earth-observation data, and rapid growth of machine learning (ML) has significantly improved landslide and slope failure-related studies, like landslide susceptibility assessment and detection (Herrera, 2016).

1.2 Problem Statements

Landslides are the most common hazards in the hilly terrain with unstable slopes and fragile geological structures. Generally, slope failure, debris flow, and landslide or mass movements are the major hazards in the watershed of hilly and mountainous regions. Each year, a huge amount of life and property is lost due to landslide hazards. Additionally, human activities like road excavation, deforestation, and mining throughout the hills destabilize the slope, causing landslides,

soil erosion, and sedimentation. These phenomena have severe impacts on vital infrastructures, including roads, houses, hydropower, and facilities for irrigation and drinking water, and also cause serious environmental degradation.

The Mai Khola watershed of Ilam District represents one of the most landslide-prone regions of eastern Nepal, where fragile geology, steep slopes, and intense monsoon rainfall combine to produce recurrent slope failures. In recent decades, the expansion of rural road networks, unplanned slope-cut excavations, and tea cultivation on steep terrain have further intensified landslide occurrence. The downstream hydropower project in Mai Khola is facing severe sedimentation due to excessive soil erosion and frequent landslides in the upstream catchment. This rapid sediment deposition reduces reservoir capacity, damages turbines, and threatens the long-term efficiency and sustainability of the project. Despite the clear hazard, systematic susceptibility assessment and zonation maps for this basin remain scarce, limiting the capacity of local authorities and communities to implement targeted mitigation. While previous studies have applied statistical models in other districts, no comprehensive evaluation integrating multi-temporal inventory data, remote sensing inputs, and comparative model validation has yet been conducted for the Mai Khola watershed. Addressing this gap is critical for providing evidence-based support to disaster risk reduction, sedimentation problems in the downstream, land-use planning, and infrastructure development in Ilam's rapidly changing mid-hill environment.

1.3 Aim and Objectives

The main objective of this study is to evaluate and map the landslide susceptibility in the Mai Khola region of Ilam District by applying a GIS-based statistical approach, thereby identifying vulnerable zones and supporting disaster risk reduction and land-use planning.

Specific Objectives

- To prepare a comprehensive landslide inventory of the study area using satellite imagery, field data, and secondary sources.
- To identify and analyze key landslide conditioning factors.
- To apply statistical approaches (Frequency Ratio and Weight of Evidence method) for landslide susceptibility assessment.
- To generate a landslide susceptibility map that categorizes the study area into different hazard levels.
- To validate the susceptibility map using historical landslide records and field verification.

1.4 Scope of the Study

- Compilation of past and recent landslide events from satellite imagery, field surveys, reports, and governmental/non-governmental databases.
- Use of validation techniques such as ROC Curve, AUC values, and success/prediction rate curves to evaluate model performance.
- Providing scientific basis for land-use planning, watershed management, infrastructure development, and disaster preparedness.

1.5 Project Report Organization

This academic project report seeks to provide a systematic understanding of the process for evaluating potential landslide risks in the Mai Khola Watershed, Eastern Nepal. It focuses on various aspects, including collecting and processing relevant data, using two different algorithms for landslide susceptibility predictions, and finally, representations of the results in GIS. The thesis follows a manuscript format with six chapters. Here's a brief overview of the content structure for each chapter.

- **Chapter 1** introduces the general background, problem statement, aims & objectives, and scope of the research. It also presents the organization of the thesis.

- **Chapter 2** provides a detailed literature review of the state-of-the-art research in landslide hazard mapping, susceptibility, vulnerability, and risk assessment.

- **Chapter 3** includes the description of the study area and research material/data. Also, it includes descriptions of landslide hazard conditioning factors and landslide inventory mapping.

- **Chapter 4** includes a detailed explanation of the overall research methodological frameworks, landslide factors selection, & procedures of different methods.

- **Chapter 5** discusses the major achievements and results of research, validations of the model & comparison of results, and necessary interpretations and general discussion of the findings.

- **Chapter 6** presents conclusions and Recommendations, including limitations & applicability.

Chapter 2 : Literature Review

2.1 Introduction

A landslide refers to the movement of materials, such as rocks and soil, sliding down the slope under the influence of gravity (Cruden, 1993b). Any failure of a slope, whether it involves soil, silt, gravel, or rocks, can be considered a landslide. So, the word "landslide" covers different kinds of movements, such as rocks falling, mud sliding, and debris flowing (Acharya, 2018). Different factors, such as heavy rainfall, earthquakes, or human activities, can trigger these movements, resulting in diverse forms of landslides.

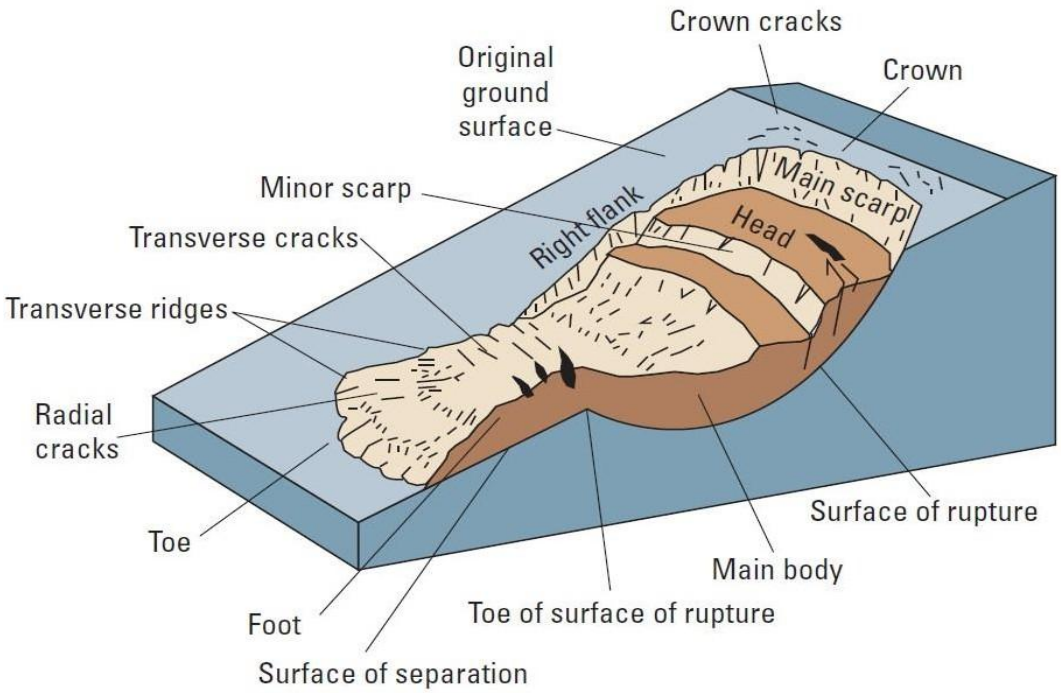

Figure 2.1: A Schematic representation of a landslide, displaying commonly used terminology for identifying the elements of a landslide

[Source: (Bobrowsky & Highland, 2013)]

2.1.1 Landslide hazard, vulnerability, and risk

Landslide hazard, vulnerability, and risk are three key concepts in understanding and managing the potential impact of landslides. Hung and Thien have undertaken a comprehensive study of Varnes' 1984 definition of landslides. Their research encompasses various aspects of hazards, risks, and vulnerability.

Landslide Hazard:

Hazard (H) refers to the probability of an occurrence of a landslide within a particular area and a specified period of time (T) (D. J. Varnes, 1984a). It considers both the spatial (geographical) and temporal (time-related) dimensions, i.e., the evaluation of landslide hazard involves foreseeing both the spatial and temporal probability. The occurrence of a landslide is typically influenced by multiple factors, including geological conditions, slope steepness, soil composition, climate, and human activities. In a more comprehensive context, the concept of hazard involves assessing both the size (area or volume) of the landslide and the likelihood of its recurrence.

Mathematically,

$$H = S * T \quad (2.1)$$

Where, S = landslide susceptibility

Vulnerability:

Vulnerability (V) represents the extent of potential harm or degree of loss experienced by a specific element or group of elements at risk within an affected area when confronted with the occurrence of a natural event of a certain magnitude. Vulnerability reflects the susceptibility to hazards and varies in terms of location, time, and individuals. It is influenced by factors such as elements at risk, population density, land use, construction practices, and the effectiveness of early warning systems (Acharya, 2018). Vulnerability assessment helps identify areas or communities at greater risk of harm in the event of a landslide.

Risk:

Landslide risk results from the combination of hazard and vulnerability, representing the potential negative consequences of a landslide event. This signifies the anticipated level of loss attributed to a particular natural event. It is often calculated as the product of the likelihood of a landslide occurrence with the potential consequences or losses (vulnerability) involved.

Mathematically,

$$R = H \cdot V \quad (2.2)$$

Understanding the risk associated with any hazard is crucial for implementing effective risk reduction measures and land-use planning.

2.1.2 Landslide Processes and Types

Landslide formation is a complex process involving a series of events that result in the downward and outward movement of materials like rock, soil, or artificial fill. Different types of landslides have different occurrence mechanisms. Landslide processes are related to slope movements or settlement, which include a continuous series of events. This results increase in shear stresses (driving forces) and a reduction in material shear strength (resisting force) (D. Varnes, 1978a) and ultimately slope fails. The safety factor (ratio of resisting to driving forces) greater than 1 indicates a safer slope, whereas less than 1 indicates an unstable slope.

Landslides are categorized by the kind of material (like rocks, dirt, debris, mud) and movement (like falling, tipping over, sliding, spreading, flowing). According to the state of activity or movement, existing landslides can be classified as active, dormant (potentially reactivated), or inactive. Landslides can be categorized based on the depth and extent of the material involved. Shallow landslides typically occur in the near-surface layers of soil and regolith (loose, fragmented material covering solid rock), and they often result from factors such as heavy rainfall, steep slopes, or changes in groundwater levels. The movement in shallow landslides is usually limited to the upper layers of the Earth's surface. On the other hand, deep-seated landslides involve not only the soil and regolith layers but also extend into the bedrock at greater depths. These types of landslides are typically larger and more complex, and they often occur along geological features like faults or fractures in the bedrock. Of all the landslide classifications, the most used classification (**Table 2.1**) was the one outlined by the late D.J. Varnes (Cruden, 1993b; D. Varnes, 1978b). This system builds upon Varnes' 1978 proposal, integrating three material types (rock, debris, and earth) and five movement types (fall, topple, slide, spread, and flow) as shown in **Fig. 2.2**.

Table 2.1: Table showing the Varnes 1978 classification of slope movements.

Type of Movement		Type of Material		
		Bed Rock	Engineering Soils	
			Predominantly Coarse	Predominantly Fine
Falls		Rock Fall	Debris Fall	Earth Fall
Topples		Rock Topple	Debris Topple	Earth Topple
Slides	Translational	Rock slide	Debris slide	Earth slide
	Rotational			
Lateral spreads		Rock Spread	Debris Spread	Earth Spread
Flows		Rock Flow (deep creep)	(Soil creep)	
			Debris Flow	Earth Flow
Complex		Combination of two or more principal types of movement		

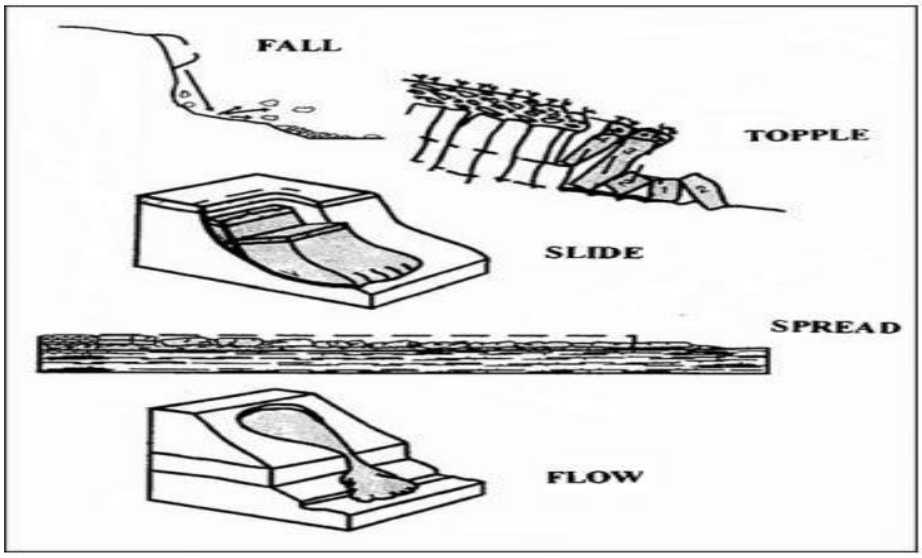

Figure 2.2: Figure illustrating types of movement defined by Cruden and Varnes,1996.

2.1.3 Landslide Causes, Effects, and Mitigation

2.1.3.1 Landslide causes and causative factors

Landslides may happen when the shear stress on a slope surpasses the shear strength of the materials comprising the slope, i.e., a factor of safety less than 1. Landslides may occur singly or in groups, numbering into the thousands. Simultaneous multiple landslides can be triggered by earthquakes, intense rainfall, or snowmelt (Guzzetti et al., 2005).

Landslides are complex phenomena influenced by various factors. Rainfall and earthquakes are the primary triggers responsible for frequent landslides throughout the world. Among the various causes, geological, morphological, physical, and human causes are the four primary causes of landslides globally (Highland & Bobrowsky, 2008). The following is the list of landslide causative factors considered by various researchers (Acharya, 2018).

- **Geomorphological factors:** elevation/altitude, relative relief, slope, aspect, general curvature (plan, profile), tangential curvature, longitudinal curvature, cross-section curvature, roughness index, topographic wetness index, stream power index, stream transportation index, slope length, diagonal length.
- **Geological factors:** lithology (texture, weathering), fault density, distance from faults/lineaments.
- **Soil factors:** soil factors include depth, drainage and hydraulic conductivity, permeability, porosity, inner texture, surface texture, slope, stoniness, effective thickness, etc.
- **Land use/cover factors**: land cover, normalized difference vegetation index, forest (type, age, diameter, and density of timber), road density, distance from road.
- **Climatic factors:** annual total rainfall, annual maximum rainfall, average annual rainfall.
- **Hydrological factors:** river density, distance from the river.

2.1.3.2 Effects of landslides

Landslides can have a range of significant effects, impacting both the natural environment and human communities. Following are some of the notable effects of landslides.

- **Loss of Life and Injury:**

Landslides can pose a direct threat to human life, causing fatalities and injuries, especially in densely populated areas or where infrastructure is affected.

- **Property Damage:**

Landslides can damage or destroy buildings, roads, bridges, and other infrastructure, leading to economic losses and displacement of communities.

- **Environmental Changes:**

The movement of large volumes of soil and rock can alter the landscape, reshape river channels, and impact ecosystems. This can result in changes to natural habitats and water courses.

- **Displacement of Soil and Debris:**

  Landslides can transport soil, rocks, and debris downslope, potentially burying areas below. This displacement can lead to long-term changes in the affected terrain.

- **Disruption of Transportation:**

  Roads and transportation networks can be disrupted or blocked by landslides, causing difficulties in mobility and the transportation of goods.

- **Impact on Water Bodies:**

  Landslides can block rivers or streams, leading to the formation of temporary dams. If these dams fail, they can trigger downstream flooding with potentially severe consequences.

- **Economic Consequences:**

  The damage to infrastructure, loss of property, and disruption to economic activities can have long-lasting economic consequences for affected regions.

- **Social and Psychological Impact:**

  Communities affected by landslides may experience social and psychological challenges, including trauma, loss of livelihoods, and the need for relocation.

- **Environmental Degradation:**

  Landslides contribute to soil erosion and degradation, affecting the quality of soil and water resources in the affected areas.

2.1.3.3 Mitigation Strategies for Minimizing Landslide Impacts

To mitigate the impact of landslides, several strategies can be employed. The Vulnerability to landslide hazards depends on factors like location, human activities, land usage, and the occurrence frequency of landslides. Alternatively, measures such as restricting, prohibiting, or imposing specific conditions on activities in hazard-prone zones can also be effective. Local governments play a pivotal role in minimizing landslide consequences by enforcing laws and rules on land usage. Avoiding building on steep slopes and in locations where landslides have already occurred, as well as improving slope stability, can further reduce the likelihood of landslides. Techniques like preventing groundwater from accumulating within the landslide mass and Safe Catching through strategies such as (1) landslide cover with an impervious membrane, (2) draining surface and groundwater from the landslide, (3) catch ditches, and(4) reducing use of surface irrigation, can effectively boost stability, etc. (Highland & Bobrowsky, 2008).

Additional methods, such as employing biotechnical slope protection techniques involving vegetated composite soil-structure, utilizing materials like soil nails and nets, along with grass seeding, can be adopted. Through these measures, the effects of landslides can be significantly mitigated, safeguarding both people and infrastructure. In order to effectively minimize the risk due to landslide hazards, commonly employed approaches include limiting development in landslide-prone areas, enforcing and adhering to construction codes, and safeguarding existing developments, and developing warning systems.

2.2 Landslide mapping and scale

A landslide hazard map results from combining spatial and temporal predictions of landslides, displaying the anticipated locations of landslide occurrences over a specific future timeframe. Landslide mapping involves the generation of different types of maps to assess and predict landslide occurrences. These include the landslide susceptibility map, vulnerability map, inventory map, and the risk map (D. Varnes, 1978b). Landslide mapping scales must be selected appropriately for landslide assessment.

2.2.1 Landslide inventory mapping

An inventory map represents past landslide locations, characteristics, and distributions over a specific area. It includes information about the surrounding area, the type, extent, and location of landslides and damage caused by them. An inventory map can give an overview of landslides that have occurred within a specific time period, but it doesn't capture long-term evolution. A polygon or a point can be used to depict landslides in an inventory map, based on the mapping scale. This map aids in understanding specific areas and predicting future landslides, yet it doesn't indicate the likelihood of failure.

Traditional methods include field mapping and visual interpretation of topographic maps, photographs, and reports. Although field mapping offers a comprehensive evaluation, it can be laborious and difficult to reach inaccessible areas. Automated and semi-automated methods use high-resolution DEM analysis, interpretation of optical remote sensing data, and analysis of Light Detection and Ranging (LiDAR) and Synthetic Aperture Radar (SAR) data for landslide inventory mapping (Guzzetti et al., 2012).

2.2.2 Landslide vulnerability mapping

In landslide vulnerability assessments, the focus is on evaluating potential losses to elements at risk using various methods such as remote sensing and GIS technology. Risk evaluation extends to considering the impacts on life, property, and the economy. Landslide vulnerability mapping is a crucial tool for identifying areas at risk of landslides and providing valuable information for risk reduction and management. Vulnerability defines the circumstances of an asset that is susceptible to a hazard. It poses challenges in landslide studies, especially in calculating social, economic, and environmental vulnerability (Rahman et al., 2022). Assessment of physical vulnerability is conducted based on the exposure level of elements at risk and the probability of loss due to landslides.

2.2.3 Landslide risk mapping

The landslide risk map shows the potential landslides in conjunction with the expected losses of life and property when a landslide occurs. Landslide risk models combine susceptibility information with vulnerability assessments, assigning quantitative values to different risk components, such as low, moderate, high, or very high risk. Different levels of risk are visualized with the help of color codes. A landslide risk map can provide valuable information for land-use planning, disaster preparedness, and emergency response efforts. It helps local authorities and communities make informed decisions to reduce the impact of landslides on both life and property.

2.2.4 Landslide Detection and Susceptibility Mapping

Many individuals tend to equate landslide detection with landslide susceptibility assessment, but there exists a notable distinction. Landslide detection and landslide susceptibility mapping are interconnected but two distinct processes (Gupta, 2022a). A susceptibility map results from the spatial prediction of landslides, showing the relative likelihood of future occurrences. It's based on analyzing the spatial links between past landslides and geo-environmental factors. This assessment entails the analysis of factors like geological characteristics, topography, and historical landslide data to anticipate areas more susceptible to future landslide events. On the other hand, Landslide detection encompasses the identification of landslide occurrences through the utilization of feature maps that depict geological attributes within a specific region of interest or by analyzing satellite images. Ground-based measurements, such as inclinometers and ground-penetrating radar, can also be used to monitor slope stability and detect potential landslide triggers. By employing a combination of these approaches, experts can enhance early warning systems, mitigate risks, and facilitate effective disaster management strategies in landslide-prone areas. Recognizing landslides, particularly in remote and challenging-to-access regions, can pose challenges due to limitations in conventional data collection techniques such as surveying and remote sensing.

2.2.5 Mapping scale

A proper scale is required for detailed landslide mapping. The scale of a map is a critical factor in determining its level of detail. Different scales are suitable for different purposes, and the choice of scales depends on the specific objectives of the mapping and the availability of data. In general, more detailed input data are needed for detailed hazard mapping. Therefore, maps of different scales, such as national scale (< 1:1000000), regional scale (1:100000 - 1:1000000); medium scale (1:25000 - 1:100000), and large scale (1:2000 - 1:25000), are prepared based on the need and data availability (BINH, 2017).

2.3 Landslide Assessment Principle and Approaches

Various approaches are employed for the assessment of landslides. **Fig. 2.1** shows a review of various methods of landslide hazard assessment. These methods rely on the assumption that areas resembling past landslide occurrences are more prone to future landslides. The landslide hazard assessment framework includes four basic levels: (a) analysis of basic information; (b) landslide danger assessment; (c) landslide hazard assessment; and (d) landslide risk assessment. Susceptibility deals with the future probability of landslide occurrence in an area (Gupta, 2022b). Most of the Landslide susceptibility studies focus on past failures to understand what could occur in the future (D. J. Varnes, 1984b). The study has grown over the years, using different methods like expert opinions or statistical analysis. Recently, machine learning (ML) techniques have been used due to their ability to handle lots of data. These techniques are learned from data to make predictions. Different ML methods like Artificial Neural Networks, Support Vector Machine, Random Forest, Logistic Regression, and Decision Trees are used, but choosing the right one is tough. People compare them based on how accurate their predictions are. Despite many studies, there isn't one best method (Marjanović, 2013a).

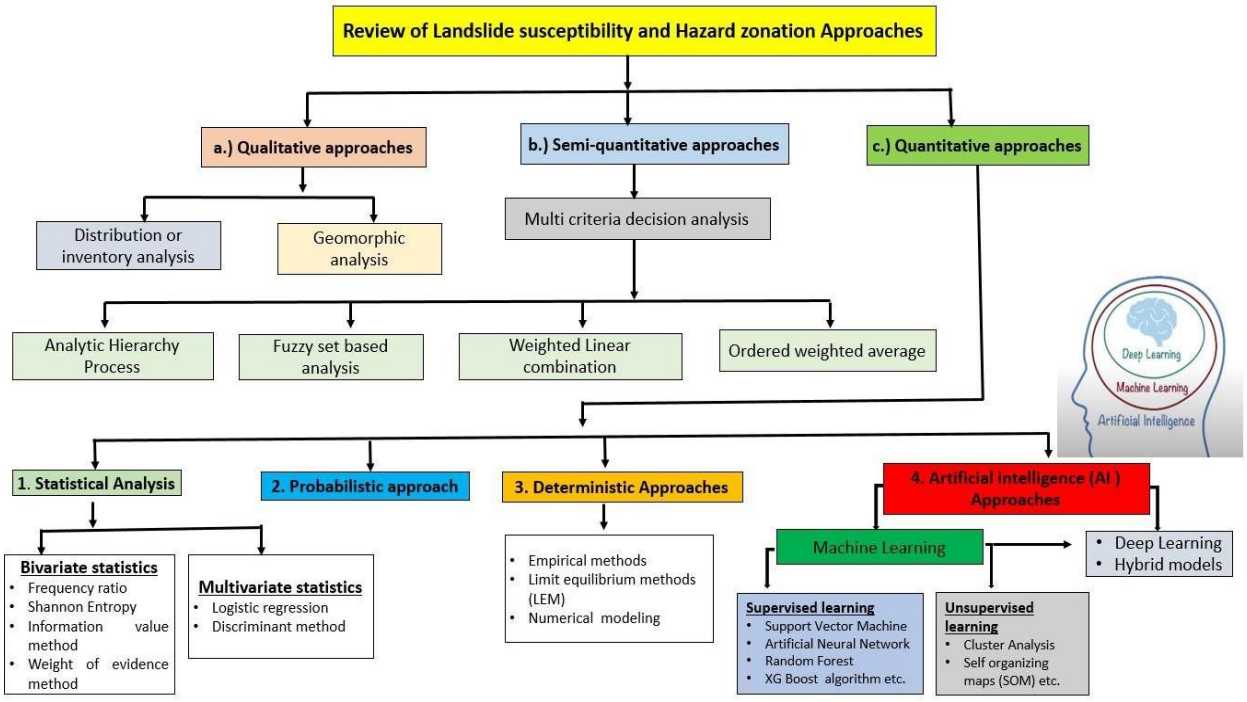

Figure 2.3: Classification of Various methods of landslide assessment and hazard zonation

The following are the most commonly used approaches for landslide hazard assessment:

2.3.1 Heuristic Approach

The heuristic approach involves using practical experience-based solutions to solve problems. Its use in landslide assessment has sparked debate; it's commonly acknowledged that heuristics are valuable for initial research (Marjanović, 2013b). They're particularly useful when detailed data is lacking, but for more accurate assessments, they can be combined with precise methods. Within this approach, various techniques exist, such as expert-opinion modeling, methods to quantify expert judgment, fuzzy/gray systems for handling uncertainty, and pattern recognition for identifying trends. Integrating these techniques can enhance the reliability of results in landslide assessment, striking a balance between practicality and accuracy. The following two are the most commonly used Heuristic methods.

2.3.1.1 Analytical Hierarchy Process (AHP)

AHP is a heuristic approach that relies on experience–based solutions and often involves expert opinions to address problems. It is useful, particularly when detailed data is lacking (Khatakho et al., 2021a). The approach consists of five distinct stages: (i) breaking down a problem into its constituent factors, (ii) organizing these factors in a ranked order, (iii) pairwise comparison (assigning numerical values that reflect the relative importance of each factor), (iv) creating a comparison matrix, and (v) computing the normalized principal Eigen vector, which gives the weight of each factor. The pair-wise comparison matrix is used to establish the priority of each factor. It gives the relative significance or likelihood of influencing factors. The Consistency Ratio (CR) is used to verify the consistency of each matrix

$$CR = CI/RI \quad (2.3)$$

Where, RI is the random index (depends on the matrix order) and the Consistency Index (CI) is computed as;

$$CI = (\lambda_{max} - n) / (n - 1) \quad (2.4)$$

where λ max is the largest eigenvalue for the n^{th} order matrix.

The Consistency Ratio (CR) serves as a tool to identify and prevent inconsistencies in the judgment matrix. Saaty (Saaty, 1990) justified that a CR below 0.1 indicates appropriate weighting

coefficients, ensuring reliable results. The weighted linear combination equation can be used to produce the landslide susceptibility index (Eq. 2.5).

$$LSI = \sum_{i=1}^{n} R_i W_i \quad (2.5)$$

where LSI denotes the landslide susceptibility index, n is the no. of factors considered, R_i and W_i indicate the rating and weightage for the i^{th} factor.

2.3.1.2 Plain Multi-Criteria Analysis (MCA)

Multi-Criteria Analysis has found successful application in landslide assessment despite its non-spatial origins. In the MCA method, systematic experts evaluate the importance of various factors influencing landslide susceptibility (F_i), such as slope angle, lithology, elevation, land use, etc., assign subjective weights (w_i) to these factors based on their perceptions, and these weights are combined with corresponding factor values to create a composite hazard susceptibility model

(Castellanos Abella & Van Westen, 2008; Marjanović, 2013b). The landslide susceptibility assessment can be done in terms of the MCA index by simply adding the weighted factors in the GIS environment, i.e.,

$$M_{MCA} = \sum_{i=1}^{n} w_i F_i = M_{AHP} \quad (2.6)$$

2.3.2 Statistical Approach

The statistical approach to landslide assessment differs from expert-based and deterministic methods as it uses available data to establish relationships between data features and landslide occurrences, introducing an objective dimension to the model. This approach does not rely on temporal predictions but focuses on spatial associations. Various techniques are employed, often determined through trial-and-error (Marjanović, 2013b). The following two are the most commonly applied statistical methods, with the frequency ratio model being a commonly utilized statistical method for landslide assessment.

2.3.2.1 Frequency Ratio Method

Frequency ratio (FR) is one of the widely used quantitative approaches for landslide assessment using spatial data in GIS. The Frequency Ratio examines the statistical relationship between landslide causative factors and landslide inventories. FR value is expressed as the ratio of landslide occurrences in a specific class to the total area of that class for the conditioning factor under consideration (Baral et al., 2021b).

$$FR = \frac{Npix(1)/Npix(2)}{\sum Npix(3)/\sum Npix(4)} \quad \ldots\ldots (2.7)$$

where,

$N_{pix}(1)$ = The number of pixels containing a landslide in a class,

$N_{pix}(2)$ = Total number of pixels of each class in the whole area,

$\sum N_{pix}(3)$ = Total number of pixels containing landslide &

$\sum N_{pix}(4)$ = Total number of pixels in the study area.

The relative frequency (RF) of the i^{th} class for the j^{th} factor is obtained using the equation given below:

$$RF = \frac{FR_i}{(\sum \mathbf{FR}_i)_j} \quad \ldots\ldots (2.8)$$

The prediction rate (PR) can be assessed through quantifying its spatial association with the training landslide datasets to establish the relative significance of each spatial factor in the available dataset (Baral et al., 2021b).

$$PR = \frac{RF_{max} - RF_{min}}{(RF_{max} - RF_{min})_{min}} \quad \ldots\ldots (2.9)$$

Where, RF_{max} & RF_{min} denote the maximum and minimum Relative Frequency among the classes within a factor, and $(RF_{max} - RF_{min})_{min}$ is the minimum value among all the factors considered.

Finally, the Landslide Susceptibility Index is obtained by combining PR and RF as:

$$LSI = \sum_i (PR_i * RF_i) \quad \ldots\ldots (2.10)$$

2.3.2.2 Weight Of Evidence Method

Bonham-Carter (1989) applied the weight of evidence model for the first time using these two calculations

$$W^{+} = \ln \frac{P(\frac{B}{D})}{P(\frac{\bar{B}}{D})} \quad \text{.....(2.11)}$$

$$W^{-} = \ln \frac{P(\frac{B}{D})}{P(\frac{\bar{B}}{D})} \quad \text{.....(2.12)}$$

In above mentioned equation, the probability is denoted by P, while ln denotes natural log. B and B respectively; represent the existence or nonexistence of potential landslide presence and absence, respectively. The above equations were modified to calculate the weight of the classes of each causal factor contributing to landslide occurrence and statistically derived using:

$$W^{+} = \ln \{(\frac{[Npix1]}{[Npix1]+[Npix2]})/(\frac{[Npix3]}{[Npix3]+[Npix4]}]\} \text{ .....(2.13)}$$

$$W^{-} = \ln \{(\frac{[Npix3]}{[Npix1]+[Npix2]})/(\frac{[Npix4]}{[Npix3]+[Npix4]})\} \text{… .....(2.14)}$$

Npix1 are the pixels that express the existence of landslides and contributing factors

Npix2 denotes the existence of landslides and the absence of contributing factors

Npix3 denotes the existence of contributing factors and the non-existence of landslides.

Npix4 shows the pixels where both landslides and landslide contributing factors are not found.

W^{c} is the final weight, which is calculated using equation below

$$W^{c} = W^{+} - W \text{..... (2.15)}$$

2.3.3 Machine Learning Approach

Machine Learning (ML) is a subset of Artificial Intelligence (AI). It is focused on training machines using data to enhance their decision-making capabilities beyond human capacity (Sreelakshmi et al., 2022). Machine learning is an emerging discipline within computer science

that uses algorithms to learn from experience. It's a mix of many subjects, like statistics, AI, and more, making it hard to put in one category.

2.3.4 Deterministic Approach

The deterministic method for studying landslides, specifically the limit equilibrium approach, is a common way to understand landslide risks. This approach is useful because it gives us numbers based on real-world rules. But we need to be careful with our data and choices to get accurate results. The deterministic approach can be integrated with geographic information systems (GIS) to analyze and visualize the results. The deterministic approach can also be applied at a regional scale to assess landslide hazard in geologically complex areas. It involves different characteristics for identifying areas prone to landslides. Although it might still use regional scales through GIS, this method demands more localized data gathered on-site and then adapted for larger regions with similar traits. Unlike earlier approaches that mainly focused on a region's geology, shape, and environment, this technique requires geotechnical details that determine the materials' mechanical properties across the area (Marjanović, 2013b). This brings the assessment closer to an engineering geological viewpoint, which is crucial on a local (specific site) level.

2.4 Review of Existing Literatures Landslide Risk Assessment and Mitigations

2.4.1 International Scale

References	Key Findings
(Dai et al., n.d.)	The article stresses systematic landslide risk assessment combining hazard probability, runout, and vulnerability. Precautions include restricting development, enforcing construction codes, slope stabilization, drainage, and warning systems. National and international experiences, such as in the U.S. and Hong Kong, show such strategies can reduce casualties and economic losses by over 90%.
(Maes et al., 2017)	The study reviews landslide risk reduction in tropical countries. It analyses 382 studies from 99 nations, finding most efforts focus on hazard assessment rather than vulnerability reduction. Recommendations stress management, education, and governance, but implementation lags due to scientific and political barriers. Overall, action remains limited despite increasing risk.
(Ward et al., 2020)	The research work reviews global natural hazard risk assessments. It shows disasters since 1990 caused 1.6 million deaths and yearly losses of USD 260–310 billion. Studies model hazards like floods, droughts, earthquakes, and landslides, comparing methods, projections, and gaps. It highlights advances, challenges, and opportunities for improved risk reduction.
(Abella & Van Westen, 2007)	This study developed Cuba's first national landslide risk index map using GIS-based multi-criteria evaluation. By combining ten hazard and vulnerability indicators, it identified Sierra Maestra and Nipe–Cristal–Baracoa as the most landslide-prone regions. The results guide disaster risk reduction, evacuation planning, and integration with Cuba's hurricane early warning system.

2.4.2 National Scale

References	Key Findings
(Devkota et al., 2013a)	The study assessed landslide risk along Nepal's Mugling–Narayanghat road using GIS-based Certainty Factor, Index of Entropy, and Logistic Regression models with 321 landslide events and twelve environmental factors. The Index of Entropy model proved most accurate (90.16%). Resulting susceptibility maps guide safer infrastructure planning, hazard mitigation, and disaster risk reduction.
(Hasegawa et al., 2009)	The article assesses landslide risks in Nepal's Lesser Himalaya through mapping, soil sampling, and shear strength testing. It identifies hydrothermal alteration and clay mineralization as key triggers. Mitigation emphasizes detailed geological and geotechnical investigations, improved road alignment planning, and consideration of landslide-prone zones during construction and maintenance to reduce monsoon failures.
(Uddin et al., 2018)	The article assesses landslide risk in Nepal using satellite data and erosion models to identify high-risk areas, especially in steep and agricultural lands. It suggests mitigation through afforestation, slope stabilization, controlled grazing, and soil conservation practices. These measures aim to reduce vulnerability, protect infrastructure, and guide safer land use planning.
(Devkota et al., 2013b)	The article reviews landslide risk assessment and mitigation globally, highlighting hazard mapping, probabilistic risk analysis, and stakeholder involvement. It stresses structural measures like slope stabilization and non-structural strategies such as land-use planning, risk communication, monitoring, and early warning systems. Technological advances, remote sensing, and international collaboration are emphasized for effective disaster risk reduction

Chapter 3 : Study Area & Data

3.1 Study Area Description

Nepal is a mountainous country located between India and China, positioned along the boundary of the Indian and Eurasian tectonic plates. The Subduction of the Indian Plate beneath the Eurasian Plate makes Nepal highly susceptible to earthquakes and the related hazards like landslides and slope failures (Okamura et al., 2015b)The general topography of the country is characterized by high relief, complex geological structures, and extreme variation of elevation from south to North. 83% of the total area lies in hilly and high mountainous regions (Acharya, 2018). The study area is located in the Ilam district of Province 1, Eastern Nepal, characterized by hilly terrain with a morphology of spur, saddle, and ridge.

The Mai Khola watershed is a sub-watershed of a larger Kankai River Basin and is a rainfed perennial river system in Eastern Nepal. The river is a major tributary of the Kankai River Basin that originates in the Sandakpur area and flows south to confluence with the Jogmai Khola. The river has a dendritic pattern with multiple small streams mixing and contributing to the river's base flow. The area is bounded by the two major south-trending spurs with a deep and narrow valley in between. During the summer monsoon, these small rivers and streams are filled with a large amount of water, which has the potential to cause flooding and other water-induced disasters. The watershed extends roughly from 26°53′N to 27°07′N latitude and 87°44′E to 88°01′E longitude and covers an area of approximately 568 km² with a perimeter of about 104 km. Elevation ranges from the Terai–Siwalik transition (~375 m) to high mid-hills exceeding 3,500 m, producing steep relief and short, high-energy catchments that drain eastwards via the Mai Khola and its tributaries.

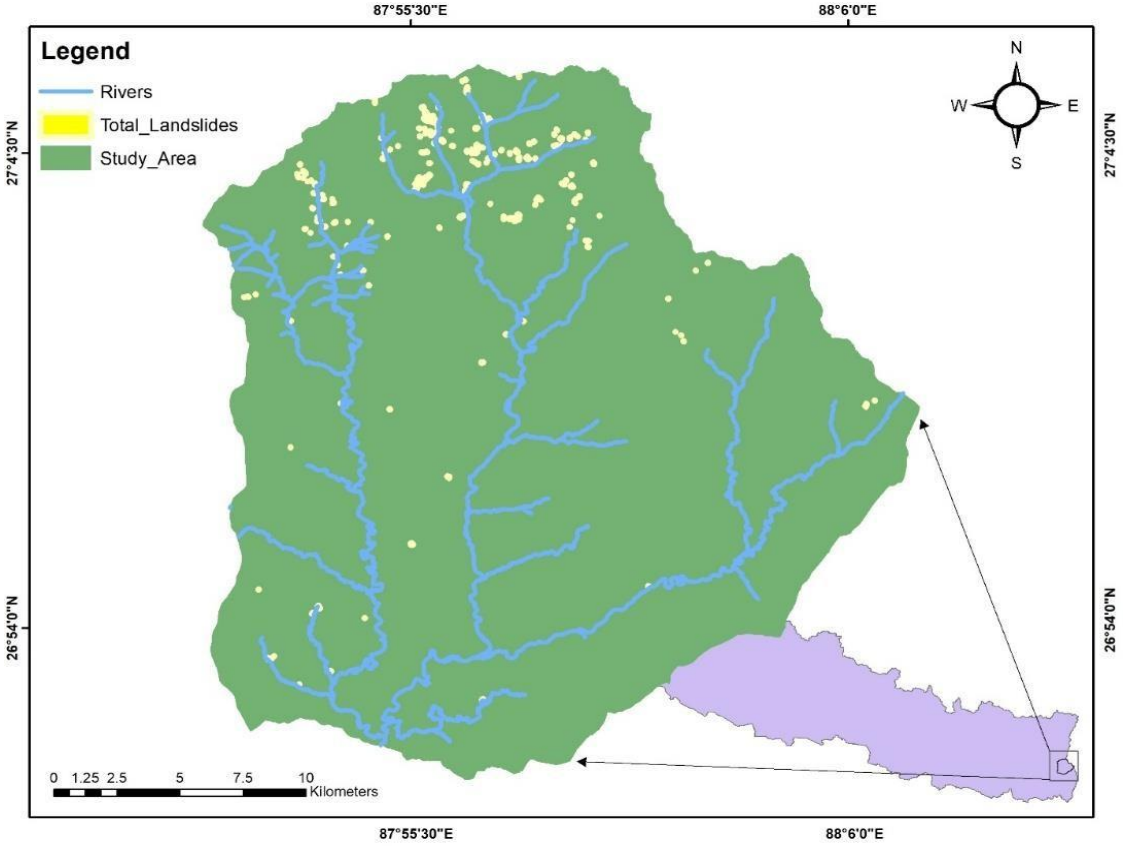

Figure 3.1: Map showing the location of the study area

3.1.1 Topography & Climate

Ilam District exhibits high topographic complexity due to its dramatic elevation range from the lowland Terai plains to steep Himalayan foothills. This rugged terrain is characterized by deeply dissected river valleys, sharp ridges, and very steep slopes, shaped by tectonic activity and intense erosion. Such variability creates significant local differences in climate, soil stability, and drainage patterns. Elevation ranges from the Terai–Siwalik transition (~375 m) to high mid-hills exceeding 3,500 m, producing steep relief and short, high-energy catchments that drain eastwards via the Mai Khola and its tributaries. Based on the national climate trends observed in Nepal, the Ilam district is experiencing significant climatic shifts characterized by a consistent rise in temperature, with warming rates estimated at 0.14°C per decade, particularly pronounced in its elevated hilly and mountainous terrains. The climate is characterized as humid subtropical to temperate, with a monsoon-dominated rainfall regime. Mean annual precipitation ranges from approximately 1,395 mm to 2,522 mm across the basin, increasing with elevation and windward exposure. Rainfall is highly seasonal (June–September), with short-duration, high-intensity convective bursts that rapidly raise pore pressures and trigger shallow slides and debris flows.

The watershed straddles the Lesser Himalayan physiographic zone, characterized by deeply incised V-shaped valleys, narrow ridgelines, and convex–concave slope profiles These morphometric conditions amplify slope instability when coupled with intense rainfall and land disturbance.

3.1.2 Geological Setting & Seismology

Bedrock belongs primarily to the Lesser Himalayan sequence, including phyllite, schist, quartzite, and gneiss, intercalated with slate and metasandstone. These lithologies weather to shallow, cohesion-variable regoliths, phyllitic and schistose units are particularly susceptible to planar shearing along foliation, while quartzites form steep, blocky slopes prone to rockfalls. Regional faulting and jointing provide pervasive discontinuities that, when daylighted on slopes, predispose to translational failures. Soil cover is thin to moderate on spurs and thicker within hollows. Clayey, silty colluvium accumulates along concave mid slopes and hollows where saturation is frequent. The mountain range is divided into five main tectonic zones. Those are Tethys Himalaya, the Higher Himalaya, the Lesser Himalaya, the Sub-Himalaya (Siwaliks), and the Indo-Gangetic Plain

(Terai). The study area lies in the Higher Himalaya zone. The Higher Himalaya and the Lesser Himalaya zones are separated by the main central thrust (MCT).

The Higher Himalayan rocks are represented by grey garnet schist, grey kyanite and sillimanite schist, banded and augen geisses with sporadic grey to light grey quartzite bands. Most of the Higher Himalayan rocks are deeply weathered, and on them are grey, brown, and yellow residual soils of more than 3 m thickness (CMS). Many large landslides are found on the Higher Himalayan rocks.

3.2 Data Collection and Analysis

A landslide is a complex process. The reliability of landslide susceptibility assessment depends on sound inventory data and causal factors. Understanding the landslide causative factors and making an inventory map are crucial steps for the assessment of landslide hazard. The accuracy of landslide susceptibility maps depends on reliable inventory and causal factors.

3.2.1 Landslide Inventory Map

Landslide Inventories are comprehensive records of past landslides in an area ,crucial for producing and validating susceptibility maps. A total of 300 past landslide locations spanning the period from 2011 to 2025 were collected as inventory data. Many of these locations were digitized using Google Earth, while the remaining few were observed through a field visit. These datasets comprise decade-long landslide events digitized in the form of polygons from Google Earth.

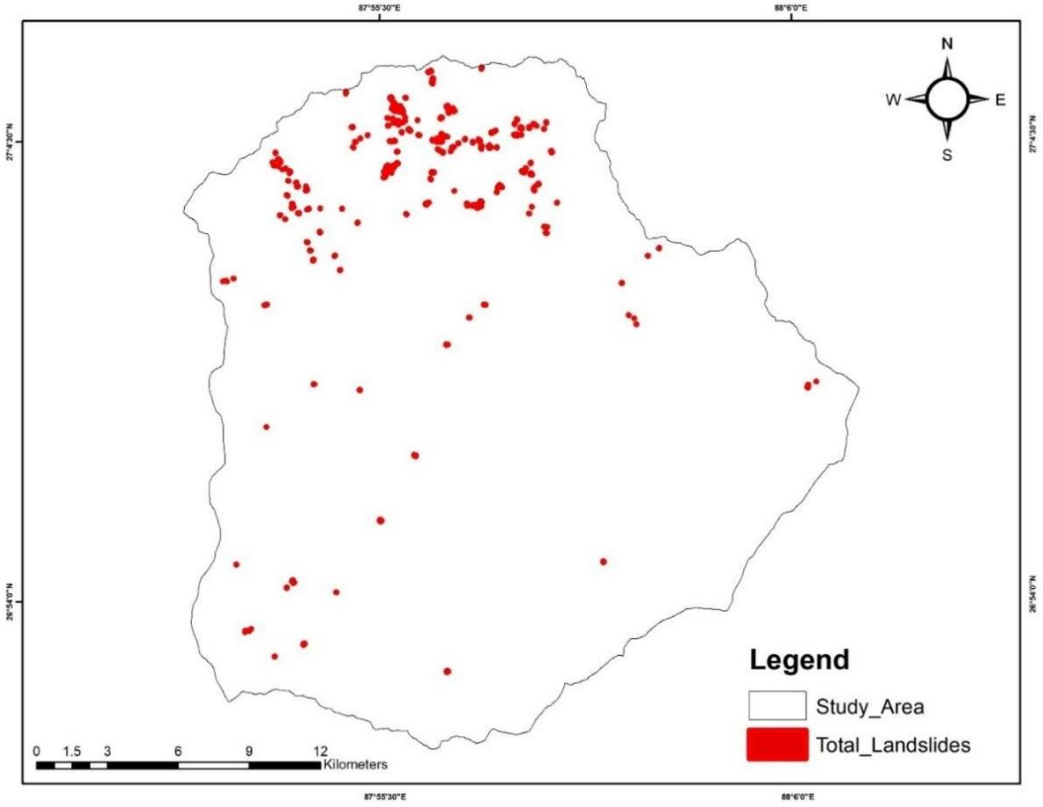

Figure 3.2: Map depicting the spatial distribution of landslide inventories in the study area

3.2.2 Digital Elevation Model and its Derivatives

A Digital Elevation Model (DEM) is a digital representation of the Earth's surface that provides elevation data for various locations (Guth et al., 2021). It is widely used in fields such as geography, cartography, hydrology, environmental modelling, and urban planning. DEMs play a crucial role in generating topographic maps, calculating slopes, identifying landforms, and assessing land susceptibility. Additionally, they can be used to derive various maps, including slope maps, aspect maps, hillside maps, and contour lines. ASTER DEM 30 m resolution was used to derive derivatives such as (Elevation, slope, aspects, curvature, and TWI) within ARCGIS.

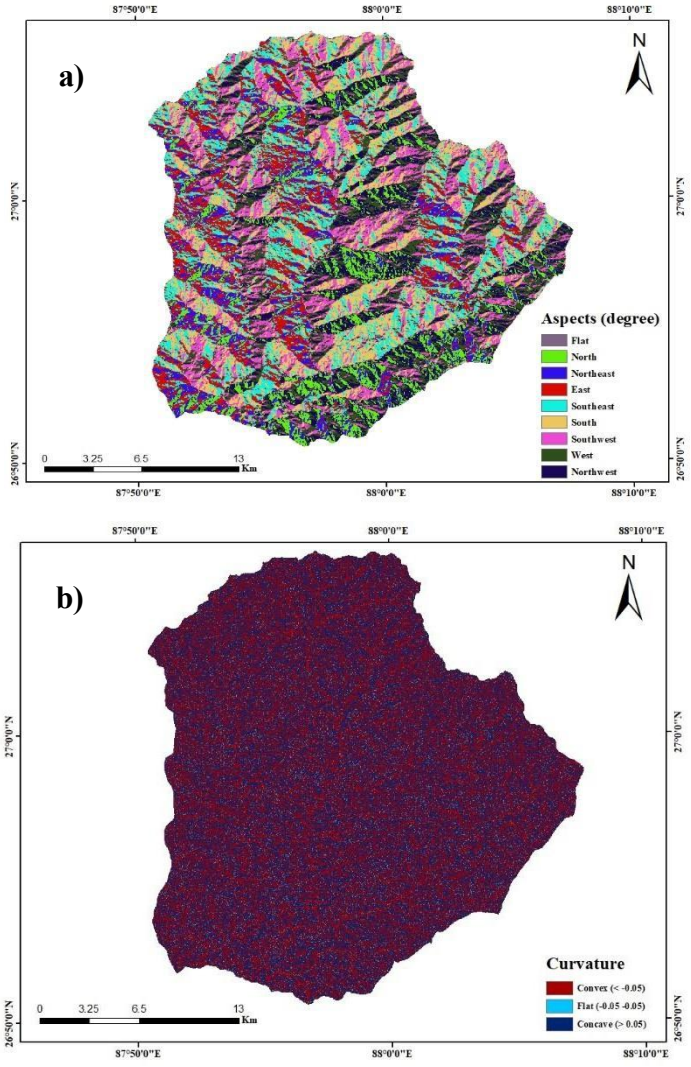

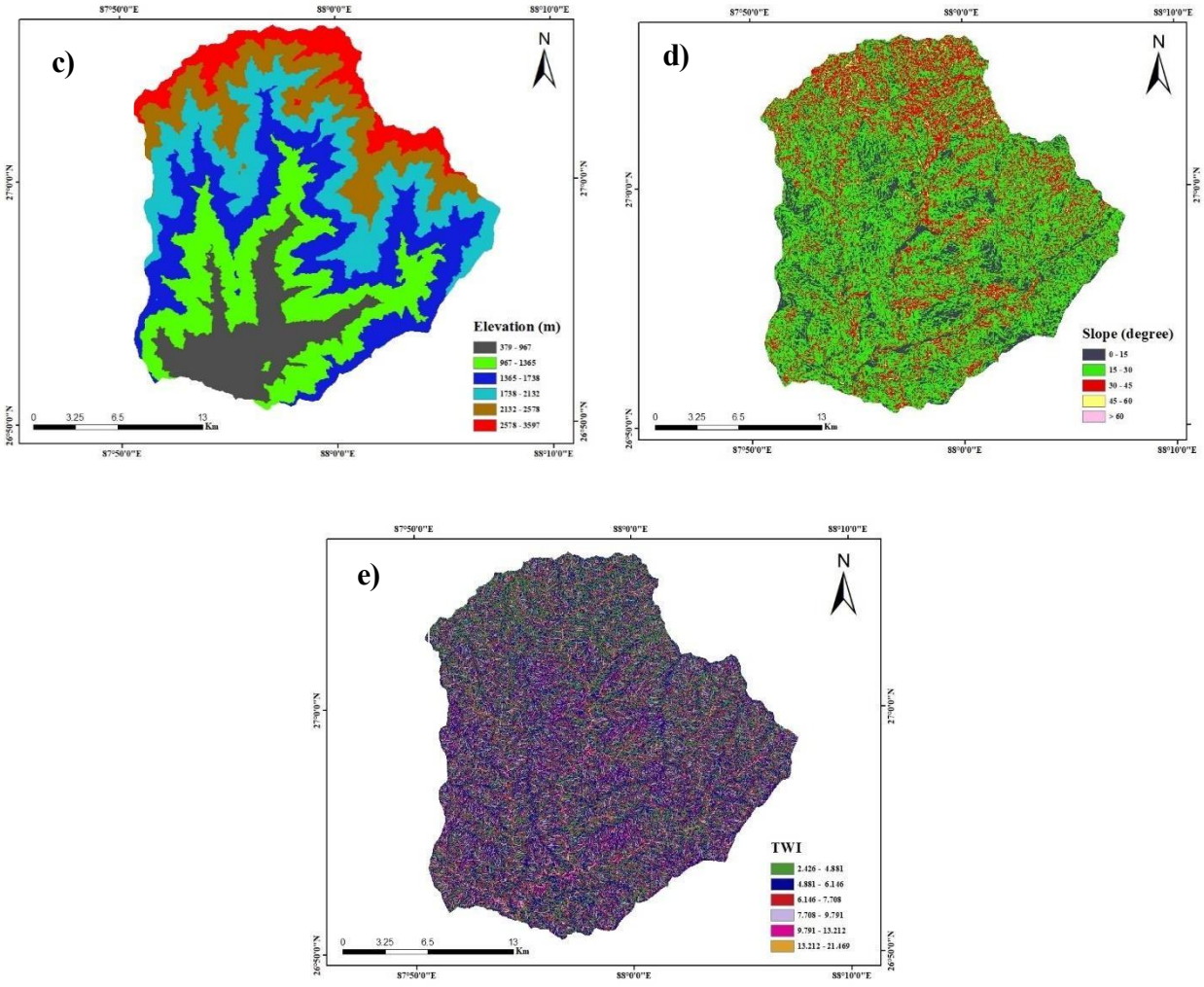

Figure 3.3: Thematic mapping of DEM & its derivatives (a) Aspects (b**)** Curvature (c) Elevation (d) Slope (e**)** TWI

3.2.3 Normalized Difference Vegetative Index

Normalized Difference Vegetation Index (NDVI) is a measure of biomass density and green vegetation. It plays a crucial role in landslide susceptibility(Khatakho et al., 2021b). Usually, the NDVI of negative values implies water bodies, 0 to 0.1 implies bare riverbeds or sandy areas and more than 0.5 implies dense vegetation cover. For this analysis, an NDVI map was produced in Google Earth Engine using Landsat satellite imagery to identify zones with insufficient vegetation that may be at higher risk of slope failure.

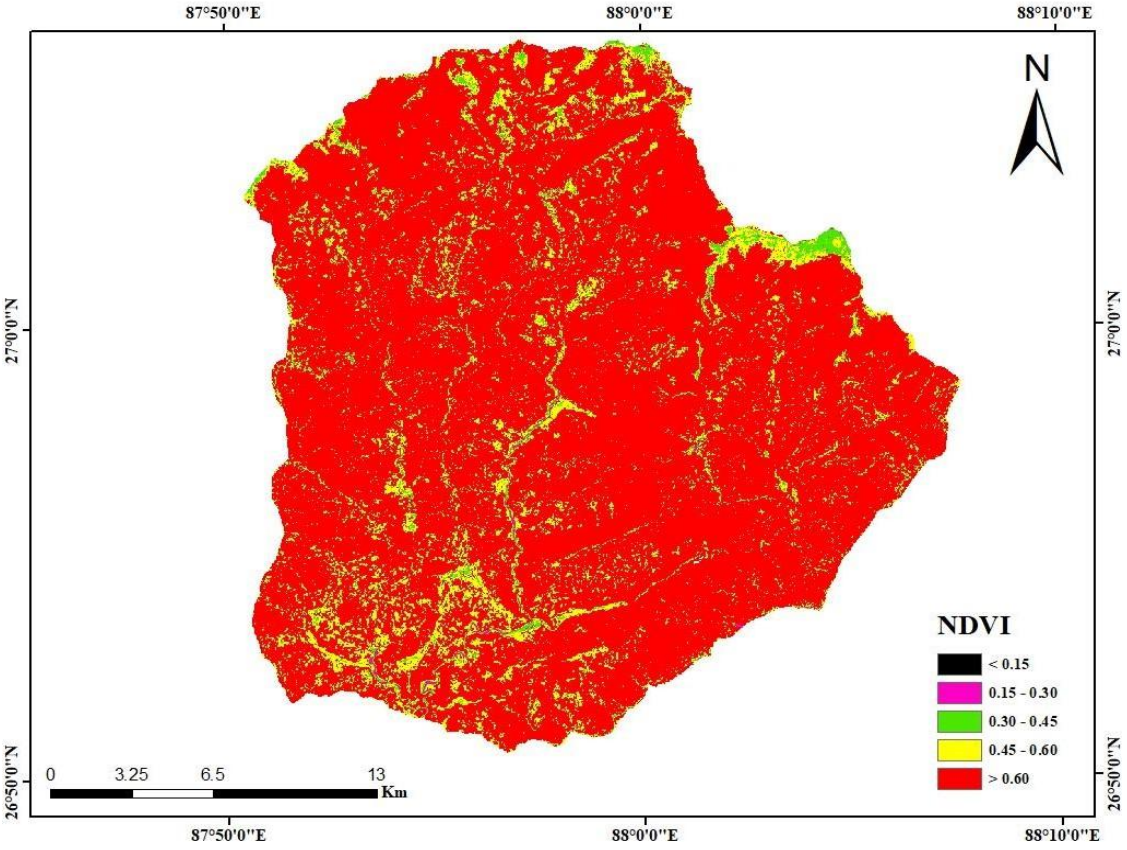

Figure 3.4: Thematic mapping of **NDVI** factor

3.2.4 Precipitation and Hydrological Data

Precipitation is the process by which water in the atmosphere condenses and falls to the Earth's surface in various forms such as rain, snow, sleet, hail, or drizzle. Precipitation data was collected as one of the key input parameters for the study, since rainfall plays a crucial role in influencing surface runoff, soil erosion, and sediment transport processes. The data was obtained from Department of Hydrology and Meteorology (DHM) Dharan, Nepal in the form of daily/monthly rainfall records for the selected stations within and around the study area. Rainfall data of total twenty rainfall stations were collected. **Table (3.1)** and **Fig (3.5)** shows the precipitation and hydrological data.

Table 3.1: Coordinates of Stations with Average Annual Rainfall data

S.N.	Station Name	Latitude	Longitude	Altitude (m)	AAR (mm)
1	Anarmani Birta	26.62506389	87.98858056	122	2565.801685
2	Chandra gadhi	26.570391	88.075144	95	2289.968371
3	Chatara	26.820435	87.159165	105	2217.8675
4	Damak	26.67066583	87.70317583	119	2294.096105
5	Dhankuta	26.98321944	87.34595556	1192	952.1738768
6	Gaida	26.65688889	87.86072222	107	2497.502083
7	Harincha	26.61000889	87.37074778	93	2091.326542
8	Himali gaun	26.88652778	88.02738889	1654	2270.610743
9	Ilam Tea Estate	26.90963889	87.92308333	1208	1395.476584
10	Kanyam Tea Estate	26.86805556	88.07833333	1570	2696.717482
11	Kechana	26.39616667	88.00375	71	2386.887337
12	Leguwa Ghat	27.15338889	87.28919444	446	870.2474012
13	Letang	26.73416667	87.50166667	256	2365.860217
14	Machhuwaghat	26.93805556	87.15472222	168	1359.789951
15	Muga	27.0500025	87.24444444	1457	1022.579286
16	pakharibas	27.04633889	87.2925	1720	1519.375
17	Sanischare	26.68972222	87.98861111	168	2589.938063
18	Tarahara	26.69881889	87.27873778	120	1970.377083
19	Tribeni	26.91424278	87.15986	146	1762.1175
20	Mulghat	26.93175	87.31969	286	1121.945641

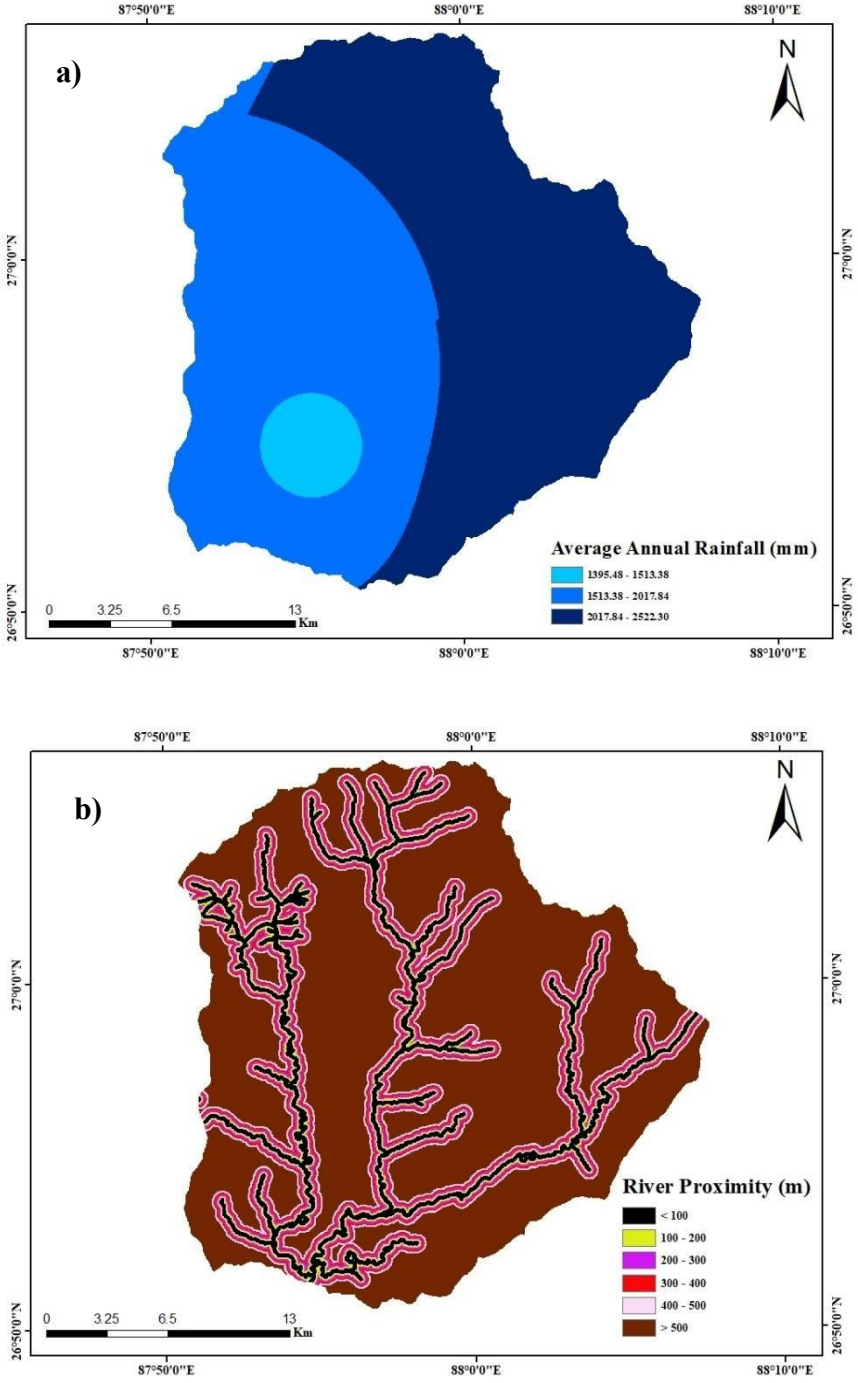

Figure 3.5: Thematic mapping of hydrological factors (a) **AAR** (b**) River Proximity**

3.2.5 Geological and Soil Data

Geological factors such as lithology, soil types can also make area prone to landslide (Ngo et al., 2021a). The geological setting strongly impacts landslide occurrence, with joints, fractures, and faults acting as triggering factors (Rahmati et al., 2019a). The assessment of landslide hazard is significantly influenced by the characteristics of the soil profile (ADPC, 2010)

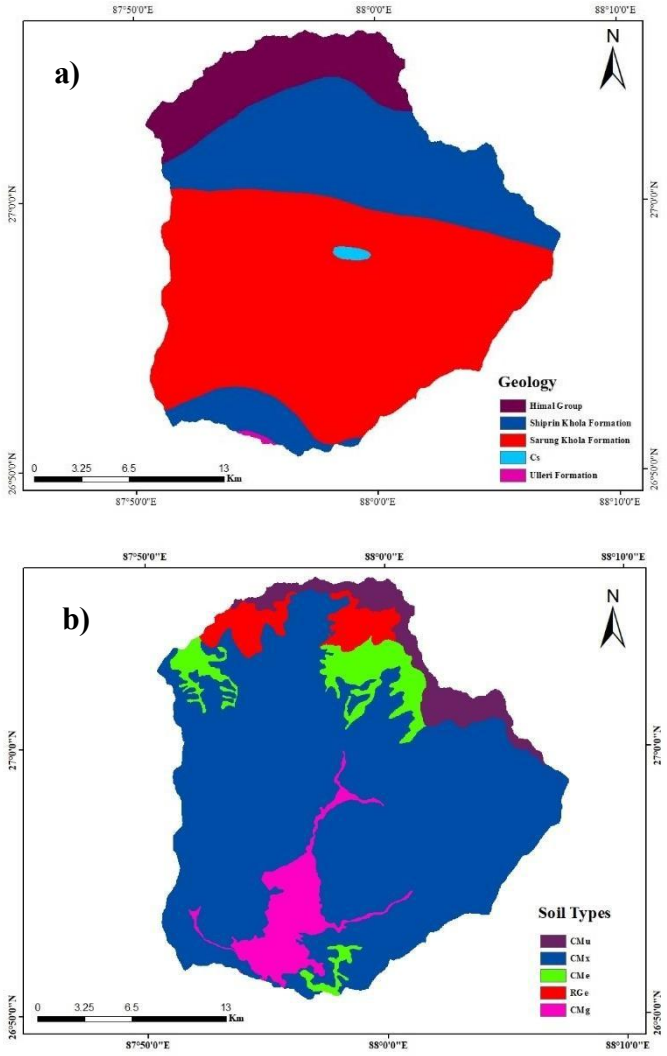

Figure 3.6: Thematic mapping of geological and soil data (a**) Geology** (b) **Soil types**

3.2.6 Roads and Infrastructure Data

Proximity to roads can significantly affect landslides by altering landscapes and soil stability (Kavzoglu et al., 2014a; Khatakho et al., 2021b). Road construction and maintenance can alter the natural landscape and contribute to changes in soil properties and stability. For example, excavation and grading during road construction can weaken slopes and increase the risk of landslides. The distance from road is inversely correlated to landslide susceptibility. Road data were digitized manually using high-resolution satellite imagery available in Google Earth Pro.These datasets typically include the location, type (e.g., paved, unpaved, trails), density, and geometry of roads, as well as other built elements like bridges, buildings, and drainage systems.

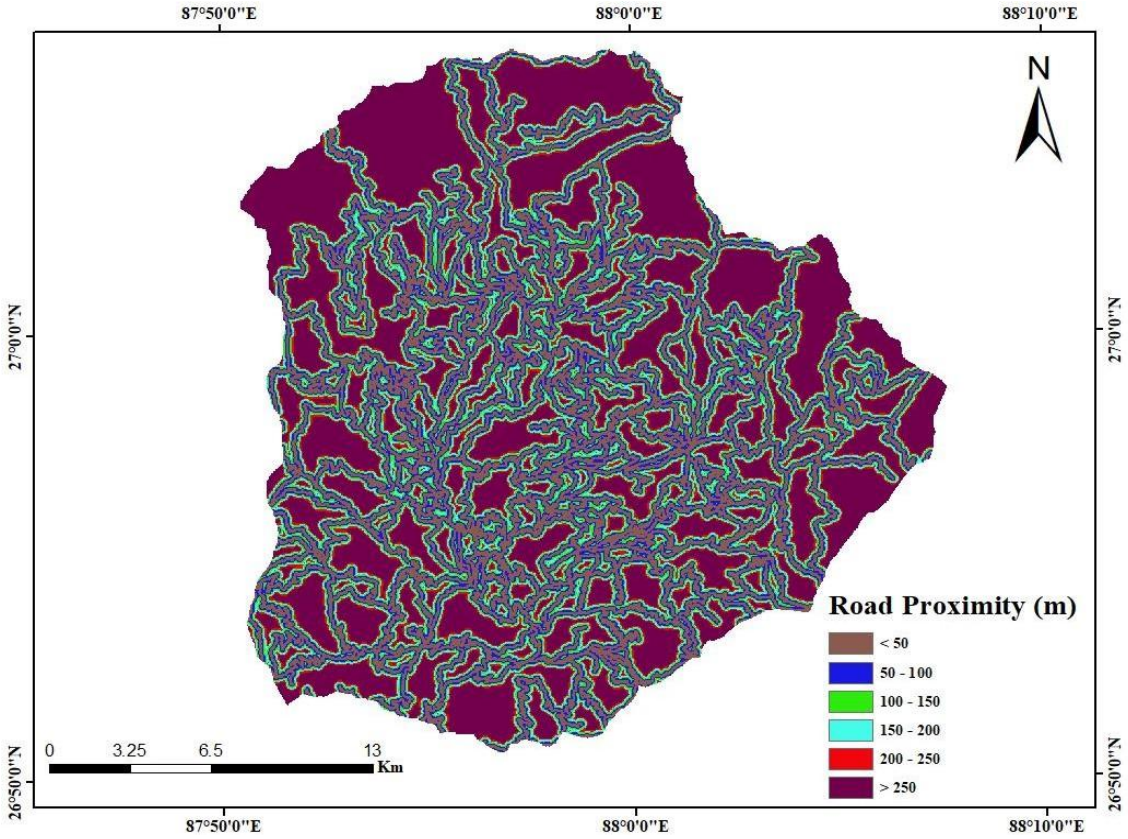

Figure 3.7: Thematic Mapping of Road Proximity

3.3 Data Sampling & Preparation

After collecting and preparing the landslide inventory and conditioning factors in GIS, a dataset consisting of factors affecting landslides and landslide labels was sampled. There are two techniques of data sampling: the pixel-based and object-based methods (Zhu et al., 2019). In this study, we applied a pixel-based method since the object-based method is quite complex. A total landslide dataset consisting of 415 pixels was sampled using GIS. The value of each landslide conditioning factor is extracted for each landslide and non-landslide pixel. Class label of '0' applied for non-landslide and '1' applied for landslide. To avoid bias, the dataset was made balanced, i.e., an equal number of non-landslide pixels was randomly sampled as that of known landslide inventory pixels. The total dataset was divided randomly into two groups: Training (80 %) and validation (20 %) data. The training dataset was used to model the landslide susceptibility of the study area, and the testing dataset was used to assess the accuracy and validation of the model.

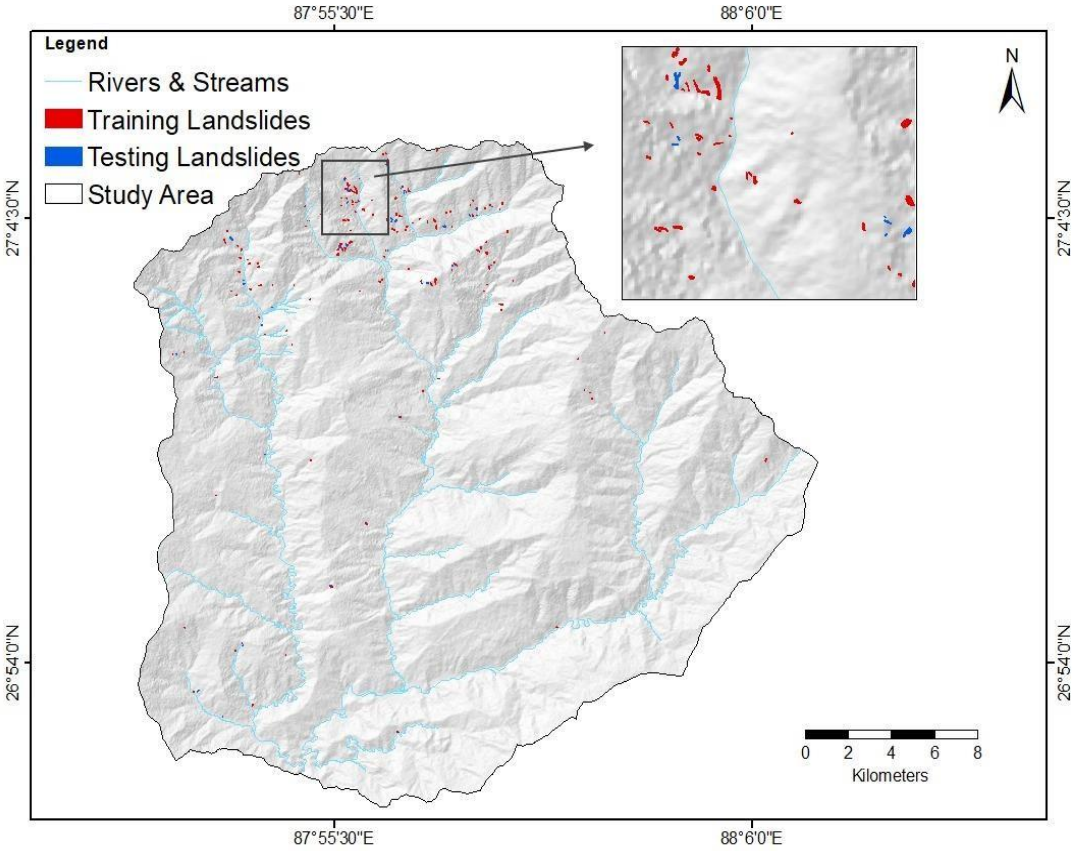

Figure 3.8: Map showing the Training and Testing dataset

Chapter 4 : Methodology

4.1 Landslide Causative Factors

Various causative factors contribute to the occurrence of landslides. Landslide causal factors and triggers are the main datasets for assessing landslide likelihood and generating susceptibility maps. Twelve landslide conditioning factors with the common spatial reference 'WGS 1984 UTM 45N' and resolution of 30m were considered based on the previous studies and the suitability of our study area. Factors such as elevation, slope, Topographic Wetness Index (TWI), aspect, and curvature were obtained using the ASTER DEM of 30m resolution. the geological data were obtained from the national geological map of 1,000,000 scale published by the Department of Mines and Geology (DMG) in 1994. The NDVI was calculated using free satellite images like the Landsat series in Google Earth Engine (GEE). Rainfall data provided by the Climate Research Unit (CRU) for the period 2000 to 2025 were used to prepare an annual rainfall map. The thematic mapping of landslide factors was done in a geographical information system (GIS) environment.

4.1.1 Geomorphological and Topographical Factors

Geomorphological factors such as Digital Elevation Model (DEM), elevation, slope, aspects, Curvature, and Topographic Wetness Index (TWI) can all influence landslide occurrence. DEM is a 3D representation of the terrain and is valuable in preparing many geomorphological derivatives for landslide assessment. Using the DEM, five geomorphological conditioning factors: elevation, slope, topographic wetness index (TWI), aspect, and curvature were generated in GIS.

a) Elevation

The effect of elevation on landslide susceptibility remains a topic of debate, and researchers have yet to provide a conclusive resolution to this issue (Kavzoglu et al., 2014b) but its indirect effects on factors like precipitation and vegetation make it widely used as a landslide factor (Ngo et al., 2021b; Rahmati et al., 2019b). High elevations often experience landslides due to steepness and unstable conditions. The elevation profile was derived from DEM and classified into six classes.

b) Slope

Slope is the rate of change of elevation over a specific horizontal distance. The velocity of flow and soil penetration are both affected by the slope angle. Areas with slopes > 5° are considered

landslide– prone (Kalantar et al., 2018). Landslides are more likely to occur on steeper slopes due to gravitational forces. The slope (in degrees) was obtained using DEM.

c) Aspect

Aspect is the compass direction that a slope faces. Aspects affect temperature and moisture, and they affect processes like hydrology and weathering (Khatakho et al., 2021b). It influences the amount of solar radiation that a slope receives, which affects the temperature and moisture content of the soil and rocks. For example, slopes that face north receive less solar radiation and are generally cooler and wetter than slopes that face south. The aspect map was prepared from the DEM and classified into nine classes.

d) Curvature

Curvature is a measure of how much a curve or surface deviates from being a straight line or a flat plane. The driving and resistive strains in the direction of mass flow are influenced by curvature. Convex slopes are stable, but concave slopes are risky due to water pressure buildup (Khatakho et al., 2021b).

e) Topographic Wetness Index

The Topographic Wetness Index (TWI) is a quantitative measure used to model and predict the spatial distribution of soil moisture and saturation zones across a landscape based on its topography. It measures water accumulation and quantifies topographic influence on hydrological processes and soil moisture. The TWI was developed by Beven and Kirkby in 1979 with in runoff model (Acharya, 2018) and is defined as:

$$\mathrm{TWI} = \ln \frac{\alpha}{\tan \beta}$$

where α represents the local upslope area draining through a specific point per unit contour length and tan β denotes the local slope.

4.1.2 Hydrological and climatic factors:

Hydrology and climate-related factors, such as rainfall and streams, are significant factors for slope instability and landslides. Rainfall is a leading trigger of landslides, causing them to occur frequently. Steam side areas are prone to slope instability due to saturation (Dai et al., 2002b).

a) Annual Precipitations

Annual rainfall refers to the total amount of precipitation (rain, snow, etc.) recorded at a specific location over a full calendar year, typically measured in millimeters (mm). Heavy and prolonged rainfall is a leading trigger of landslides. The probability of a landslide will rise as mean precipitation increases. The average annual data of the period from 2001 to 2024.

b) Proximity to streams

The landslide risk increases for the areas adjacent to the river networks because the soil materials near rivers are usually saturated and are more susceptible to slope instability due to bank erosion, undercutting, and elevated pore water pressure from the fluctuating river levels. This proximity was quantitatively integrated into their landslide hazard model using buffer zones(Dai et al., 2002b; Khatakho et al., 2021b).

4.1.3 Geological and soil Factors:

Geological factors such as lithology, soil types can also make an area prone to landslides (Ngo et al., 2021a).

a) Geology

Geology is the scientific study of the Earth's physical structure, materials, processes, and history. It is a critical factor in the landslide susceptibility model by evaluating lithological strength and proximity to tectonic features.

The geological setting strongly impacts landslide occurrence, with joints, fractures, and faults acting as triggering factors (Rahmati et al., 2019a).

b) Soil types

Soil types are categories of soil with distinct characteristics that result from a combination of five key factors: climate, organism, topography, parent material, and time. The assessment of landslide hazard is significantly influenced by the characteristics of the soil profile (ADPC, 2010).

4.1.4 Anthropogenic Factors

The occurrence of landslides is influenced by various causative factors, including human activities (Froude C Petley, 2018b). Factors like Land cover, vegetation index, road constructions, etc., alter landscapes and slope stability (Khatakho et al., 2021b; Pacheco Quevedo et al., 2023).

a) Proximity to roads

Proximity to roads can significantly affect landslides by altering landscapes and soil stability (Kavzoglu et al., 2014a; Khatakho et al., 2021b). Road construction and maintenance can alter the natural landscape and contribute to changes in soil properties and stability. For example, excavation and grading during road construction can weaken slopes and increase the risk of landslides. The distance from the road is inversely correlated to landslide susceptibility.

b) Normalized Difference Vegetation Index

The Normalized Difference Vegetation Index (NDVI) is a measure of biomass density and green vegetation. It plays a crucial role in landslide susceptibility(Khatakho et al., 2021b). Usually, the NDVI of negative values implies water bodies, 0 to 0.1 implies bare river beds or sandy areas and more than 0.5 implies dense vegetation cover.

4.2 Landslide susceptibility assessment Approaches and modeling

Several approaches to landslide susceptibility zoning have been proposed in scientific literature. These approaches can be grouped into qualitative or quantitative categories. Qualitative methods rely on researchers' theoretical and empirical knowledge to make scientific judgments, while quantitative methods establish relations between past events and their controlling factors using Statistical Models (Titti et al., 2021). The robustness and quality of results can be affected by the availability and quality of landslide inventories, although more data doesn't always guarantee better result.

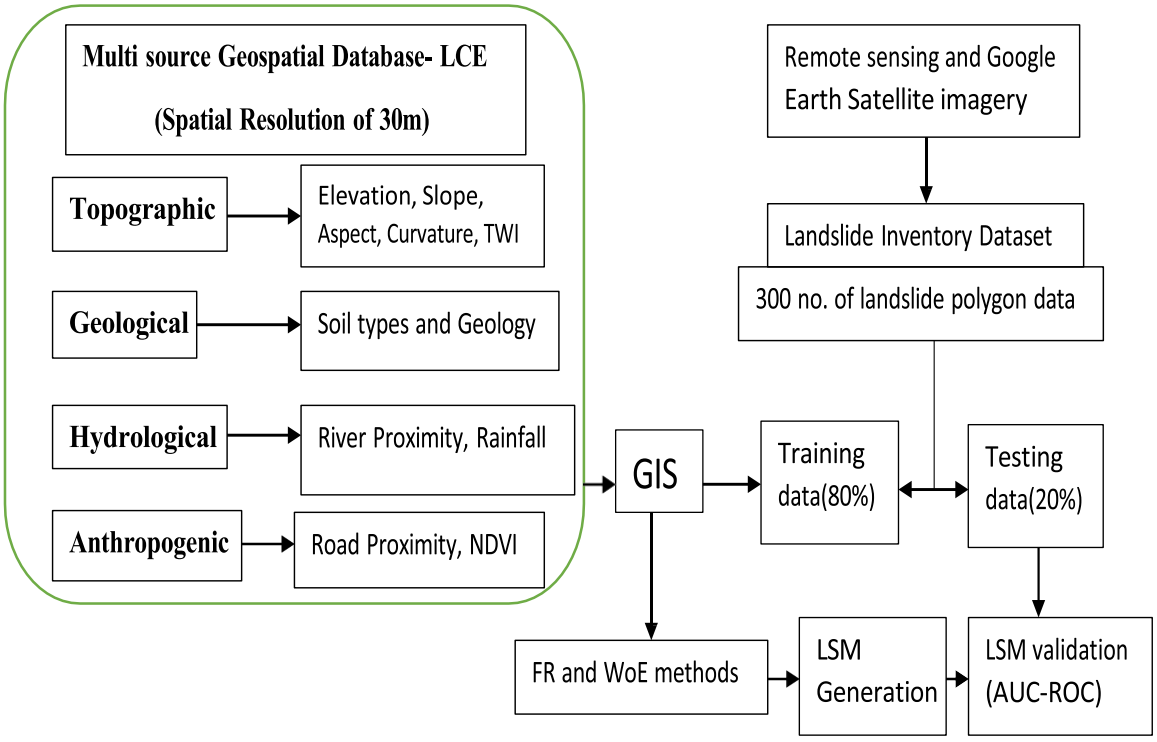

Figure 4.1: Flowchart showing the Methodological framework of the study

4.2.1 Frequency Ratio Method

The Frequency Ratio (FR) is a bivariate statistical method that quantifies the probabilistic relationship between the spatial distribution of landslides and each class of a landslide conditioning factor (Lee & Pradhan, 2007). It operates on the principle that future landslides are more likely to occur under conditions similar to those that led to past landslides.

The FR value for a specific class within a factor (e.g., slope class of 30-40°) is calculated as the ratio of the probability of landslide occurrence in that class to the probability of the areal extent of that class in the entire study area. Mathematically, it is expressed as:

$$\mathbf{FR} = \frac{\mathrm{Npix(1)/Np\dot{x}(2)}}{\sum \mathrm{Np\dot{x}(3)}/\sum \mathrm{Npix(4)}} \quad \text{(2.7)}$$

where,

$N_{pix}(1)$ = The number of pixels containing a landslide in a class,

$N_{pix}(2)$ = Total number of pixels of each class in the whole area,

$\sum N_{pix}(3)$ = Total number of pixels containing landslide &

$\sum N_{pix}(4)$ = Total number of pixels in the study area.

The relative frequency (RF) of i^{th} class for j^{th} factor is obtained using the equation given below:

$$\mathrm{RF} = \frac{FR_i}{(\sum \mathbf{FR}_i)_j} \quad \text{(2.8)}$$

The prediction rate (PR) can be assessed through quantifying its spatial association with the training landslide datasets to establish the relative significance of each spatial factor in the available dataset (Baral et al., 2021b).

$$\mathrm{PR} = \frac{\mathrm{RF_{max}} - \mathrm{RF_{min}}}{(\mathrm{RF_{max}} - \mathrm{RF_{min}})_{\min}} \quad \text{(2.9)}$$

Where, RF_{max} & RF_{min} denote the maximum and minimum Relative Frequency among the classes within a factor, and $(RF_{max} - RF_{min})_{min}$ is the minimum value among all the factors considered.

Finally, the Landslide Susceptibility Index is obtained by combining PR and RF as:

$\mathrm{LSI} = \sum_i (PR_i * RF_i)$

The resulting continuous LSI values were classified into five susceptibility zones (Very Low, Low, Moderate, High, Very High) using a natural breaks (Jenks) classification scheme in ArcGIS to produce the final susceptibility map.

4.2.2 Weight of Evidence Method

The Weight of Evidence (WoE) is a Bayesian probability-based statistical method used to describe the spatial relationship between a set of landslides (the "training points") and conditioning factors (Bonham-Carter, 1994). In this context, “evidence" is the presence of a specific factor class that makes a landslide more or less likely.

For each class within each factor, two weights are calculated:

$$W^{+} = \ln \frac{P(\frac{B}{D})}{P(\frac{B}{D})}$$

$$W^{-} = \ln \frac{P(\frac{B}{D})}{P(\frac{B}{D})}$$

In above mentioned equation, the probability is denoted by P, while ln denotes natural log. B and B respectively represent the existence or nonexistence of potential landslide presence and absence, respectively. The above equations were modified to calculate the weight of the classes of each causal factor contributing to landslide occurrence and statistically derived using:

$$W^{+} = \ln \{(\frac{[Npix1]}{[Npix1]+[Npix2]})/(\frac{[Npix3]}{[Npix3]+[Npix4]}]\}$$

$$W^{-} = \ln \{(\frac{[Npix3]}{[Npix1]+[Npix2]})/(\frac{[Npix4]}{[Npix3]+[Npix4]})\}$$

Npix1 are the pixels that express the existence of landslides and contributing factors.

Npix2 denotes the existence of landslides and the absence of contributing factors,

Npix3 denotes the existence of contributing factors and the non-existence of landslides.

Npix4 shows the pixels where both landslides and landslide contributing factors are not found. W^{c} is the final weight which is calculated using the equation below,

$$W^c = W^+ - W$$

4.3 Model Evaluation and Performance Analysis

Assessing and validating the generated model is a challenging endeavor. Model evaluation examines how well a predictive model performs and the quality of its results. A common approach involves a confusion matrix, which reveals true and false counts in predictions. The model's overall performance can be assessed using the Receiver Operating Characteristic (ROC) curve, a technique applied in this study as well. It is a commonly used graphical representation that provides a clear and intuitive way to assess the accuracy of classification (Acharya, 2018). It shows the relationship between sensitivity (true positive) and 1- specificity (false positive), allowing easy visual evaluation. The ROC curve is determined by AUC, which measures the accuracy of training and validation sets. It ranges from 0.5 to 1, with a value greater than 0.5 indicating the model's validity and acceptability.

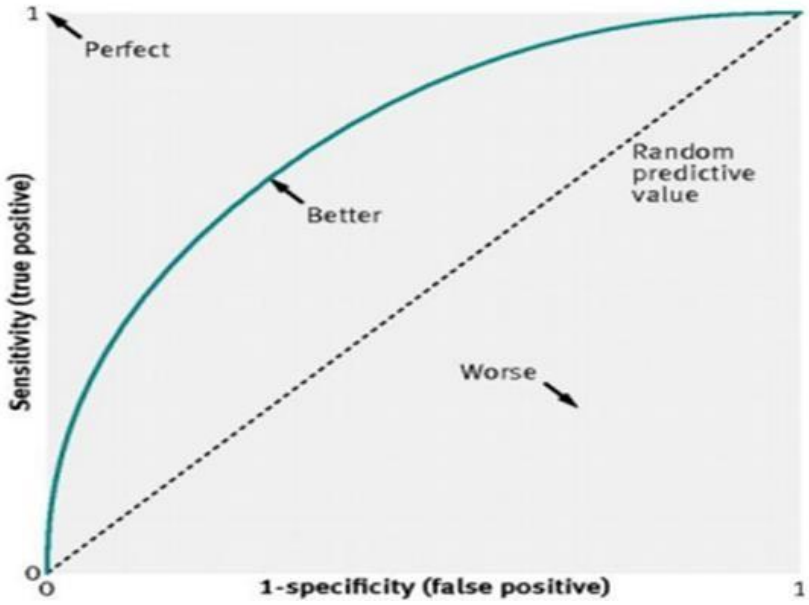

Figure 4.2: Illustration of Receiver-operating characteristic (ROC) curve

According to Amare (Amare et al., 2021), based on AUC ML- model can be categorized as **Table 4.1,** and the Precision, Recall, F1-score, and Accuracy of the model computed as given in **Table 4.2.**

Table 4.1: Model classification based on AUC (after Amare et al., 2021)

SN	AUC (%)	Model classification
1	AUC < 50	Very poor, unacceptable
2	50 ≤ AUC < 70	Poor, unacceptable
3	70 ≤AUC < 80	Good acceptable
4	80 ≤ AUC < 90	Very good
5	≥ 90	Excellent

Table 4.2: Formula for calculation of model performance

SN	Performance matric	Formula
1	Precision	$\frac{TP}{TP + FP}$
2	Recall	$\frac{TP}{TP + FN}$
3	F1-score	$2 * \frac{Precision * Recall}{Precision + Recall}$
4	Accuracy	$\frac{TP + TN}{TP + TN + FP + FN}$

[Where, TP: True Positives, TN: True Negatives, FP: False Positives, and FN: False Negatives]

4.4 Tools and Software

To accomplish the objectives of this research, several software tools and platforms were employed for data acquisition, processing, analysis, and documentation. The major tools and software used are outlined below:

- **ArcGIS**: A comprehensive Geographic Information System (GIS) software used for spatial data management, geoprocessing, map generation, and preparation of thematic layers essential for landslide susceptibility analysis.
- **Google Earth**: Utilized for visual inspection of terrain, interpretation of topographical features, delineation of landslide-prone areas, and verification of spatial datasets.
- **Microsoft Excel**: Employed for data tabulation, organization, and statistical analysis. It was also used for generating graphs, charts, and preliminary data comparisons.
- **Mendeley**: Adopted as a reference management tool for systematic organization of academic literature, proper citation formatting, and bibliography management.
- **Google Scholar**: Served as the primary academic search engine for retrieving peer-reviewed research papers, reports, and other scholarly resources relevant to the study.
- **Basic Software Utilities (MS Word, MS PowerPoint, etc.)**: These were used for report writing, formatting, and presentation preparation to effectively communicate the outcomes of the research.

Chapter 5 : Result & Discussion

5.1 Landslide Causative Factor Mapping

Landslide causative factors mapping is the process of identifying and spatially representing the natural and human-induced factors that influence slope instability. These factors include **topographical and geomorphological**, **hydrological and rainfall , geological and soil , and anthropogenic .**By mapping these variables in a GIS environment, researchers can analyze their relationship with past landslide occurrences and prepare landslide susceptibility maps, which help in risk assessment, land-use planning, and disaster management.

5.1.1 Topographical & Geomorphological Factors

These are related to the shape and features of the land. Steep slopes, weak slope angles, slope aspect (direction), elevation, and land curvature affect how stable a hillside is. For example, very steep slopes or concave slopes are more prone to failure because gravity easily pulls soil and rocks downward.

The mapping results show that landslide susceptibility is mainly influenced by slope aspect, curvature, and water accumulation. Moist, north-facing, concave slopes with high TWI values are highly vulnerable, while drier, south-facing, flat, and convex slopes remain relatively stable. The elevation map shows terrain variation from 379–3597 m, while the slope map reveals gradients ranging from 0–>60°. Both significantly influence landslide susceptibility, with steep slopes and higher elevations being more vulnerable.

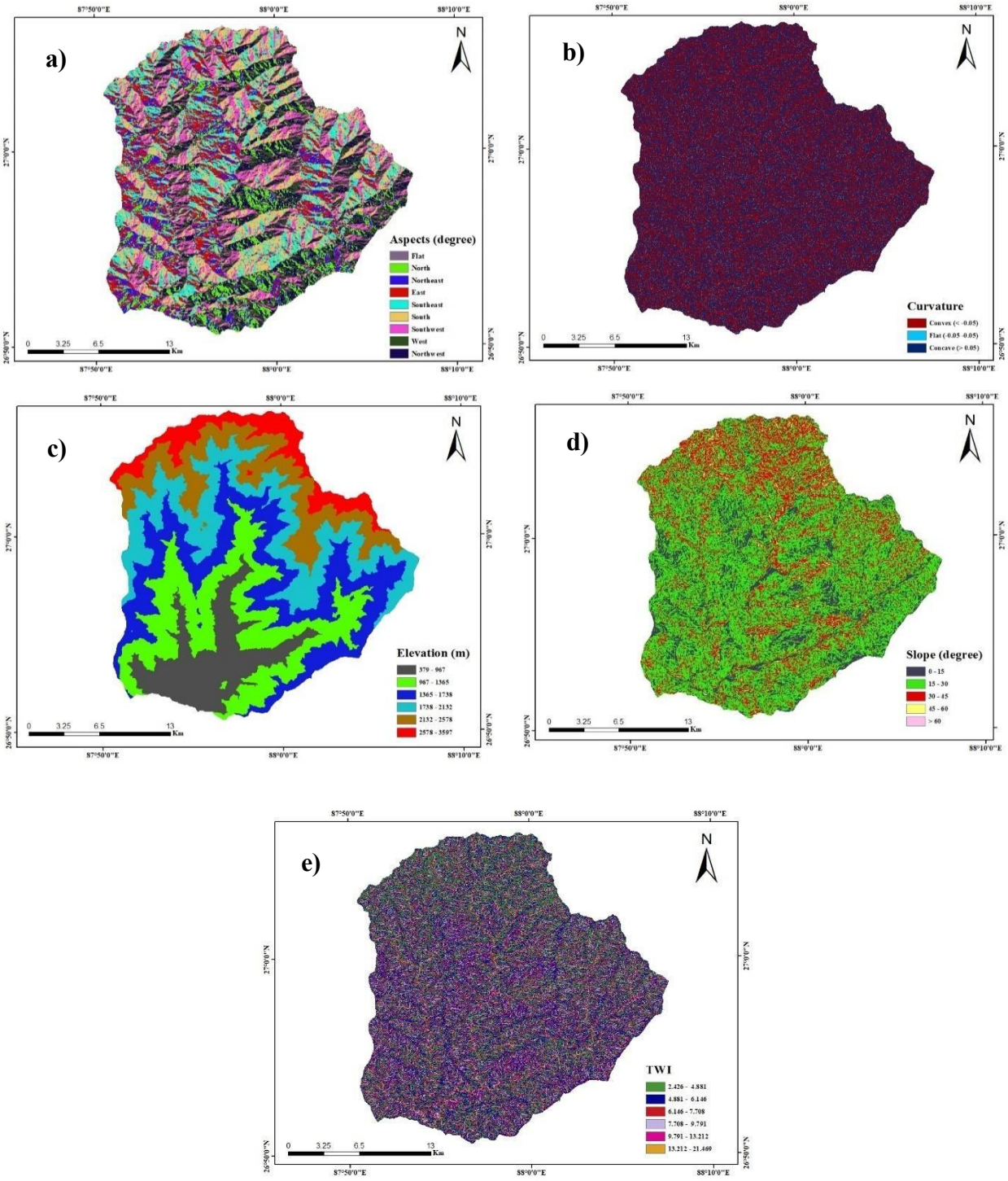

Figure 5.1: Thematic mapping of (a) Aspects (b) Curvature (c) Elevation (d) Slope (e) TWI

5.1.2 Hydrological & Rainfall Factors

These include rainfall, drainage patterns, groundwater conditions, and wetness index. Mapping them helps show how water seeps into soil, increases its weight, and reduces stability especially during heavy monsoon rains. The average annual rainfall map shows spatial variation from 1395–2522 mm. Higher rainfall zones, mainly in the eastern region, intensify landslide susceptibility due to increased soil saturation and slope instability. Proximity to rivers impacts landslide susceptibility. Areas within 100 meters have high risk due to erosion, while those farther away (200-500 meters) show moderate to low risk, depending on other factors.

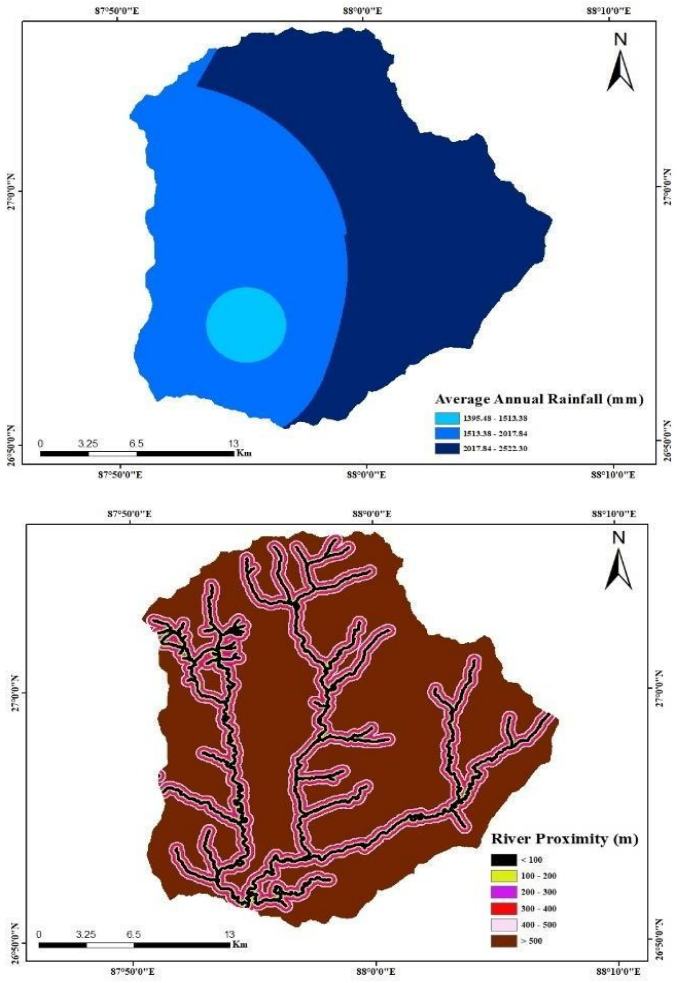

Figure 5.2: Thematic mapping of Average Annual Rainfall & River Proximity

5.1.3 Geological & Soil Factors

These maps highlight rock types, faults, soil types, and weathering conditions. Weak rocks, clay-rich soils, and earthquake-prone areas are marked as high-risk for landslides. The mapping shows diverse soil types and geological formations across Mai Khola Watershed. Central areas have unstable soils and weak geology, increasing landslide susceptibility, especially where Sarung Khola Formation and RG_e soils dominate.

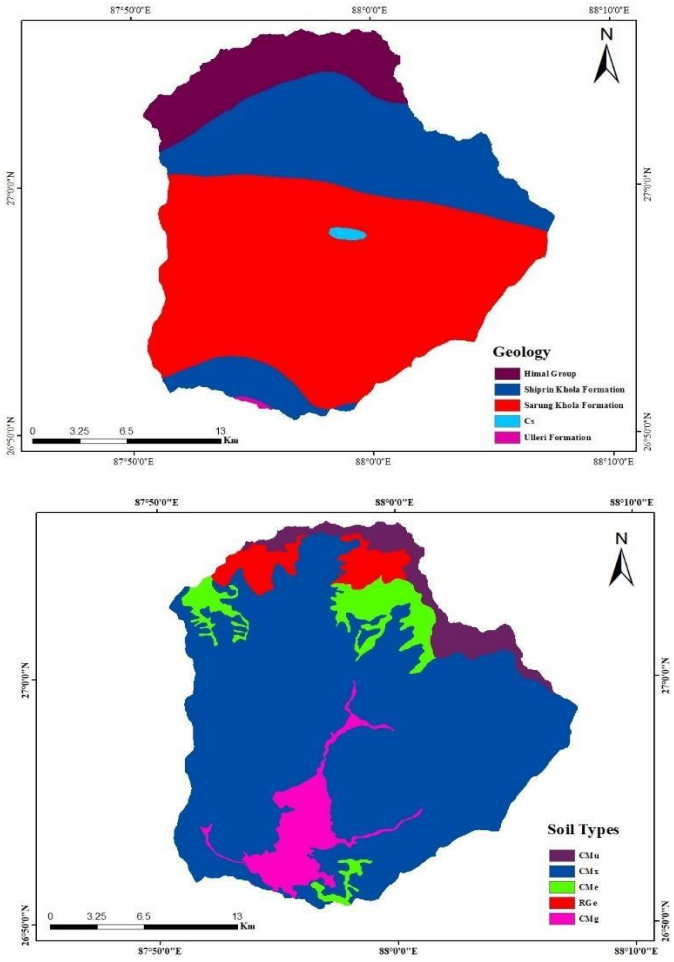

Figure 5.3: Thematic mapping of Geology & Soil types

5.1.4 Anthropogenic Factors

These maps focus on land use/land cover, deforestation, road cutting, mining, and settlements. Human changes to slopes often accelerate landslide risks by disturbing natural stability. The maps show that areas with low vegetation (NDVI < 0.15) and close proximity to roads (<50 meters) are more susceptible to landslides. High vegetation cover (NDVI > 0.60) and distance from roads reduce landslide risk.

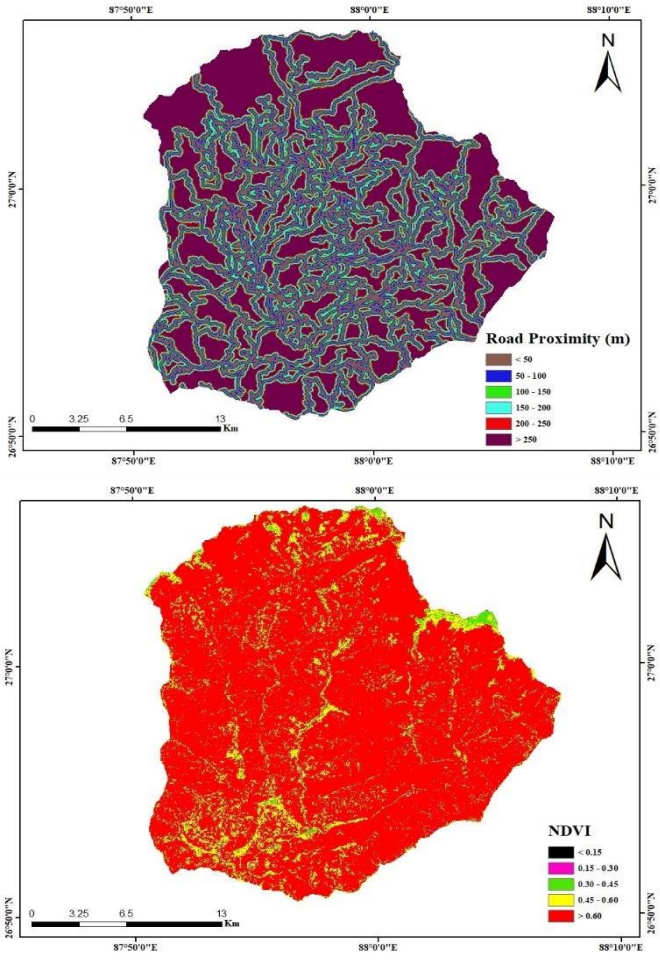

Figure 5.4: Thematic mapping of Road Proximity & NDVI

5.2 Landslide Hazard Assessment

A susceptibility map results from the spatial prediction of landslides, showing the relative likelihood of future occurrences. Predicting future landslides involves studying spatial connections between past occurrences and geo-environmental factors. Such a type of mapping work acts as an initial step towards disaster mitigation. In this study, two commonly used statistical methods were applied for susceptibility prediction and mapping of the study area.

5.2.1 Landslide Susceptibility Mapping (LSM) using Frequency Ratio and Weight of Evidence Methods

In the study area, Landslide Susceptibility Mapping (LSM) was conducted using two bivariate statistical methods: Frequency Ratio (FR) and Weight of Evidence (WoE). Both methods analyzed the relationship between past landslides and conditioning factors, producing susceptibility maps with five categories: very low, low, moderate, high, and very high.

Frequency Ratio (FR): This method compared the proportion of landslide pixels to total area pixels, with values >1 indicating higher susceptibility. The FR-based map showed a clear link between past landslides and high FR zones.

Weight of Evidence (WoE): Based on Bayesian probability, this method calculated positive and negative weights for each factor class, highlighting the relative contribution of each class to landslide occurrence. The WoE based map also showed strong alignment between high-contrast zones and past landslides.

Both methods validated the identified landslide-prone areas and provided reliable susceptibility maps.

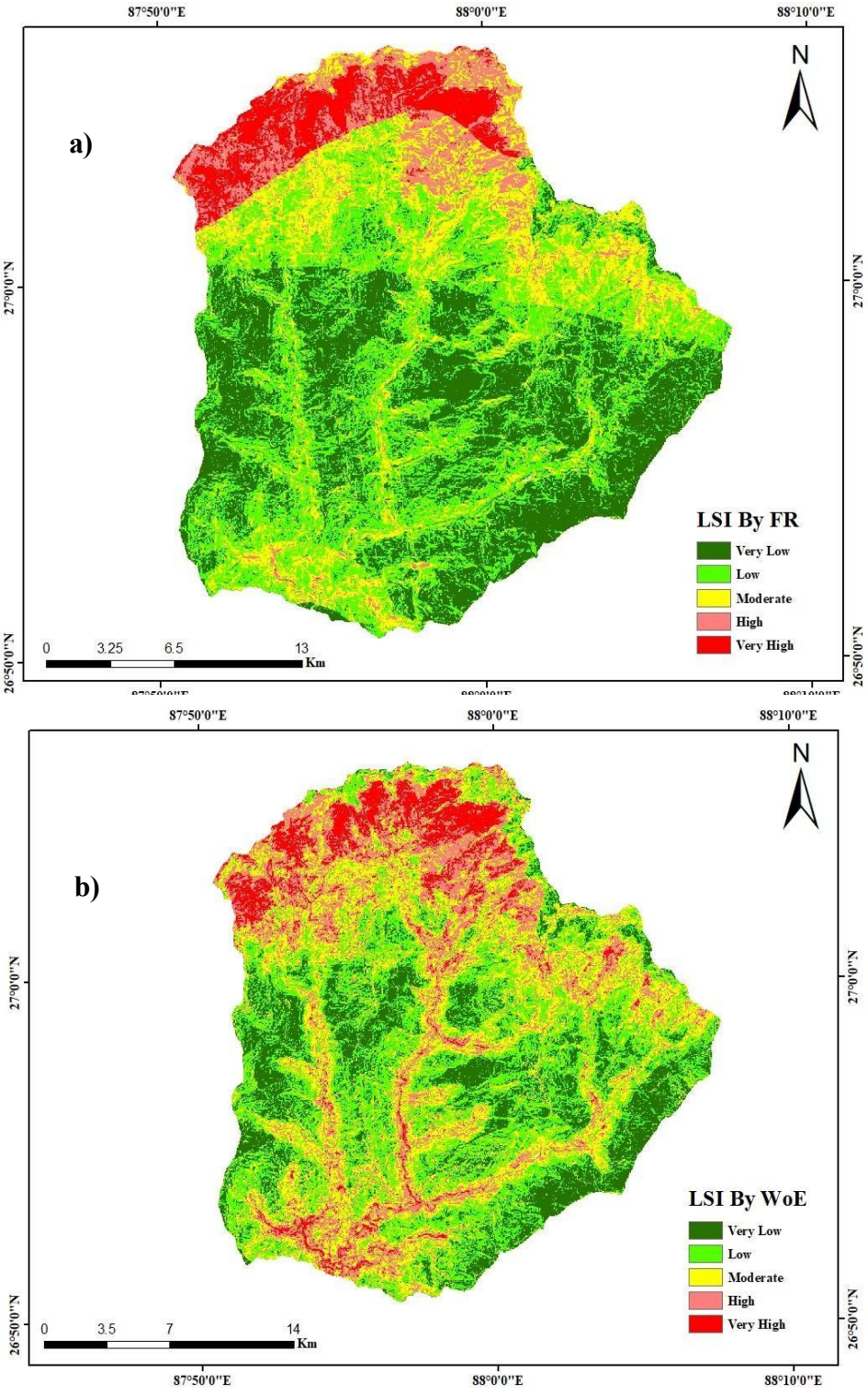

Figure 5.5: Landslide Susceptibility Mapping Using (a) FR Method & (b) WoE Method

5.2.2 Spatial Pattern and Interpretation of both models.

Table 1.1: Percentage of area of landslides under different risk categories

S N	Landslide Risk	% Area of land under different risk categories of Landslides	
		FR model	WoE model
1	Very Low (VL)	31	18.17
2	Low (L)	35.34	30.695
3	Moderate (M)	19.242	26.484
4	High (H)	8.466	17.889
5	Very High (VH)	5.94	6.76

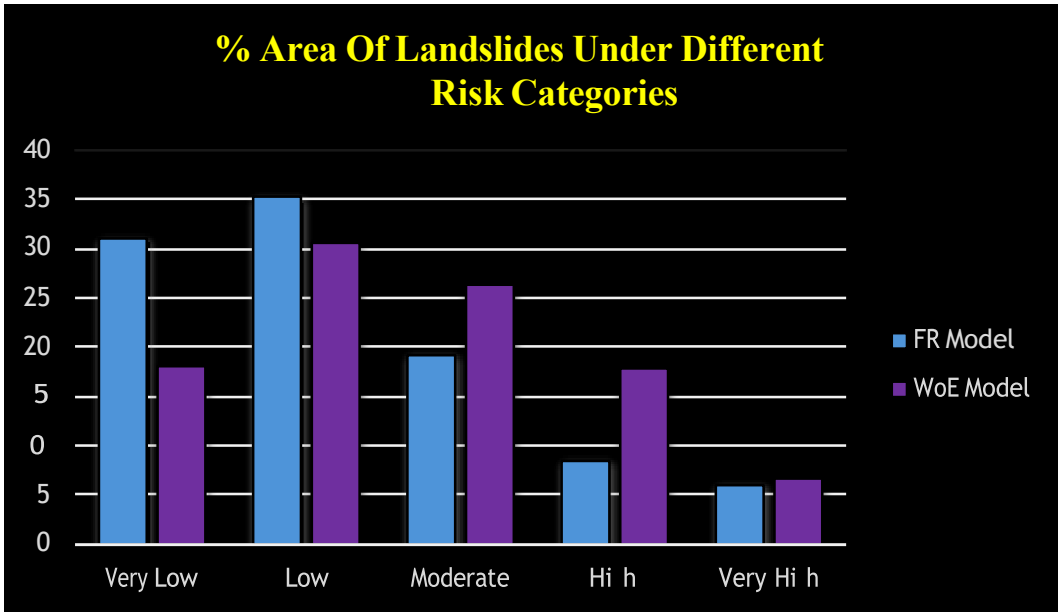

Figure 5.6: Percentage of area of landslides under different risk categories.

The application of the Frequency Ratio (FR) model successfully generated a landslide susceptibility map (LSM) for the study basin, categorizing the entire area into five distinct classes: Very Low, Low, Medium, High, and Very High. The subsequent areal statistics provide a critical quantitative assessment of the basin's susceptibility distribution.

The analysis reveals that the majority of the basin is characterized by low susceptibility. Cumulatively, the Low and Very Low susceptibility classes encompass 66.34% of the total basin area, indicating that a substantial portion of the region is relatively stable and has a lower probability of landslide occurrence. In contrast, a significant and concerning portion of the basin is classified as highly susceptible. The High (8.47%) and Very High (5.94%) susceptibility zones together account for 14.41% of the total area. These high-risk zones, while less extensive, represent critical areas that are highly prone to slope failures and demand prioritized attention for hazard mitigation strategies. The remaining 19.25% of the basin area is classified as possessing a Medium level of susceptibility, representing a transitional zone where the likelihood of landslide occurrence is moderate.

This distribution underscores a landscape where widespread stability is punctuated by specific, highly vulnerable areas. The concentration of a significant percentage of land into the high and very high categories, despite their smaller areal extent, is a common and critical finding in landslide susceptibility studies, as these zones often correlate with steep slopes, specific geological formations, and proximity to existing landslide activity.

The Landslide Susceptibility Mapping (LSM) using the Weight of Evidence (WoE) model produced a robust zonation of the basin, classifying the terrain into five distinct classes: Very Low, Low, Medium, High, and Very High. Areal statistics reveal that the High (17.88%) and Very High (6.76%) susceptibility classes collectively encompass 24.64% of the total basin area. This indicates that nearly a quarter of the study area is characterized by a high propensity for slope instability, a finding that necessitates prioritized risk management interventions. The remainder of the basin is classified as predominantly Low/Very Low susceptibility, with a transitional Medium class, outlining a clear spatial distribution of hazard potential.

5.3 Model Validation and Performance Analysis

Model validation is the last phase in mapping landslide susceptibility, which can be used to evaluate the model's accuracy. The predictive performance of the Weight of Evidence (WoE) model was rigorously validated using the Receiver Operating Characteristic (ROC) curve. The analysis's findings are displayed in (**Fig. 5.7**).

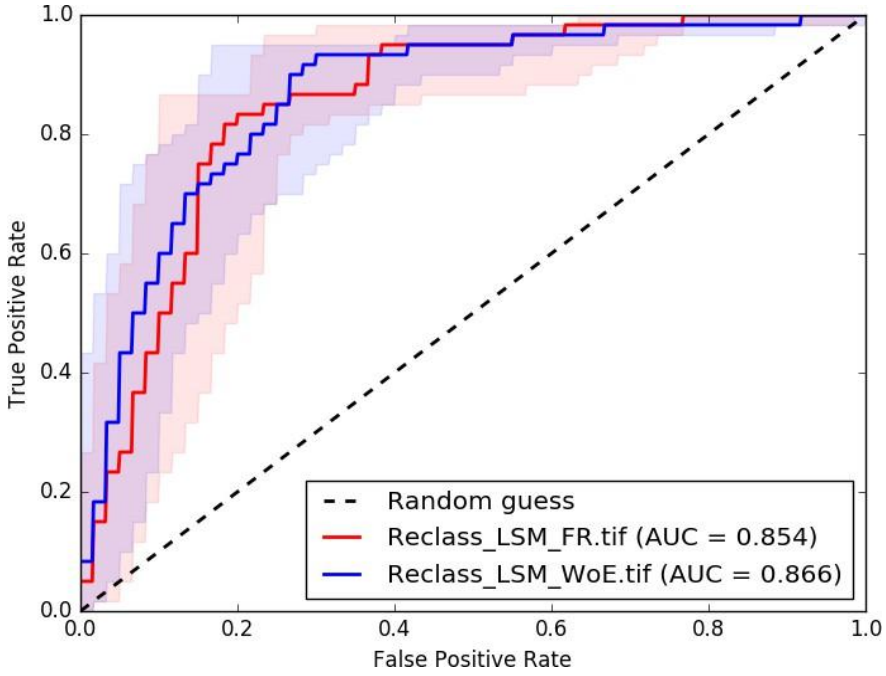

Figure 5.7: ROC curve comparing the AUC value of both statistical models

The results demonstrate that both models performed exceptionally well:

- **Frequency Ratio (FR) Model** Achieved an AUC of **0.854.**
- **Weight of Evidence (WoE) Model** achieved a higher AUC of **0.866.**

According to the standard classification for predictive accuracy (Hosmer & Lemeshow, 2000), an AUC value between 0.8 and 0.9 indicates "very good" performance. Therefore, both models are highly accurate, with the WoE model showing superior predictive ability for this specific study area and dataset.

The high AUC values validate the entire methodological framework, including:

1. The completeness and accuracy of the landslide inventory.
2. The selection of appropriate and significant causative factors.
3. The correctness of the model computations.

The superior performance of the WoE model can be attributed to its probabilistic foundation, which more effectively handles the complex spatial relationships between multiple landslide conditioning factors and reduces the overestimation bias that can occur in FR.

5.4 Results

The FR model shows that landslide probability increases with slope angle, peaking between 30°–60°. Aspect strongly influences susceptibility, with southern, eastern, and southeastern slopes being more prone, while northwestern slopes are least affected. Convex slopes, proximity to streams (<100 m) and roads (<50 m), and NDVI values of 0.15–0.30 show the highest landslide correlation. Geologically, the Himal Group (phyllites, slates, schists, dolomites) is most vulnerable due to weak, weathered rocks, whereas the Sarung Khola formation is least susceptible. These findings highlight slope angle, aspect, geology, vegetation cover, and proximity to streams and roads as dominant controls on landslide occurrence. The WoE analysis revealed that slope angles of 30°–45°, southern aspects, and convex curvatures have the strongest positive correlations with landslides, indicating their dominant role in slope instability. Proximity to rivers (<100 m) and the Himal Group formation, composed of weak metamorphic rocks, also showed high weight contrast values, reflecting their strong influence on failure processes. Additionally, soils such as RGe and CMe, low vegetation cover (NDVI <0.15), and elevations between 379–967 m were found to be highly susceptible zones. These factors collectively demonstrate that landslide occurrence is strongly controlled by terrain morphology, geology, vegetation, and hydrological proximity, confirming that landslides cluster in areas where these critical conditions overlap

.

Table 5.2: Landslide causative factors and Frequency Ratio Values

SN	LCF	Class	class pixels counts	% class pixels (P(s))	Landslide pixel counts	% Landslide pixels (b)	FR
1	AAR (mm)	1395.48 - 1513.38	25659	0.040788	17	0.040964	1
		1513.38 - 2017.84	282041	0.44834	179	0.431325	0.96
		2017.34 - 2522.30	321378	0.510871	219	0.527711	1.03
2	Geology	Himal Group	74906	0.119079	115	0.277108	2.33
		Shiprin Khola Formation	192139	0.305446	137	0.33012	1.08
		Sarung Khola Formation	358962	0.570646	163	0.392771	0.69
		Cs	2104	0.003345	0	0	0
		Ulleri Formation	934	0.001485	0	0	0
3	Soils Types	CMu	37229	0.059183	5	0.012048	0.2
		CMx	484031	0.76947	284	0.684337	0.89
		CMe	38813	0.061701	56	0.13494	2.19
		RGe	27952	0.044436	50	0.120482	2.71
		CMg	41020	0.06521	20	0.048193	0.74
4	Slope (°)	0 - 15	128826	0.204797	22	0.053012	0.26
		15 - 30	356339	0.566479	209	0.503614	0.89
		30 - 45	136156	0.21645	174	0.419277	1.94
		45 - 60	7693	0.01223	10	0.024096	1.97
		> 60	28	4.45E-05	0	0	0
5	Elevation (m)	379 - 967	85333	0.135655	68	0.163855	1.21
		967 - 1365	139158	0.221222	85	0.204819	0.93
		1365 - 1738	141716	0.225289	36	0.086747	0.39
		1738 - 2132	125100	0.198874	75	0.180723	0.91
		2132 - 2578	90532	0.14392	133	0.320482	2.23
		2578 - 3597	47203	0.07504	18	0.043373	0.58
6	Curvature	convex (< - 0.05)	303337	0.482221	222	0.53494	1.11
		Flat (- 0.05 - 0.05)	22945	0.036476	11	0.026506	0.73
		Concave (> 0.05)	302760	0.481303	182	0.438554	0.91

Table 5.2: Continued

7	Aspects (°)	Flat (-1)	16	2.54E-05	0	0	0
		North (0 - 22.5; 337.5 - 360)	50929	0.080963	3	0.007229	0.09
		Northeast (22.5 - 67.5)	51848	0.082424	31	0.074699	0.91
		East (67.5 - 112.5)	82487	0.131131	66	0.159036	1.21
		Southeast (112.5 - 157.5)	96929	0.15409	84	0.20241	1.31
		South (157.5 - 202.5)	104953	0.166846	124	0.298795	1.79
		Southwest (202.5 - 247.5)	91899	0.146094	72	0.173494	1.19
		West (247.5 - 292.5)	79344	0.126135	32	0.077108	0.61
		Northwest (292.5 - 337.5)	70637	0.112293	3	0.007229	0.06
8	NDVI	< 0.15	18	2.86E-05	0	0	0
		0.15 - 0.30	1746	0.002776	7	0.016867	6.08
		0.30 - 0.45	13859	0.022033	46	0.110843	5.03
		0.45 - 0.60	69680	0.110779	90	0.216867	1.96
		> 0.60	543698	0.864383	272	0.655422	0.76
9	TWI	2.426 - 4.881	199249	0.31675	139	0.33494	1.06
		4.881 - 6.146	224200	0.356415	148	0.356627	1
		6.146 - 7.708	122341	0.194488	72	0.173494	0.89
		7.708 - 9.791	56408	0.089673	36	0.086747	0.97
		9.791 - 13.212	20582	0.03272	17	0.040964	1.25
		13.212 - 21.469	6262	0.009955	3	0.007229	0.73
10	Proximity_roads (m)	< 50	137897	0.219203	124	0.298795	1.36
		50 - 100	98081	0.155911	63	0.151807	0.97
		100 - 150	74850	0.118983	65	0.156627	1.32
		150 - 200	49206	0.078218	32	0.077108	0.99
		200 - 250	49932	0.079373	29	0.06988	0.88
		> 250	219118	0.348313	102	0.245783	0.71
11	Proximity_rivers (m)	< 100	54456	0.086564	91	0.219277	2.53
		100 - 200	43942	0.069851	52	0.125301	1.79
		200 - 300	44966	0.071479	59	0.142169	1.99
		300 - 400	37921	0.06028	34	0.081928	1.36
		400 - 500	39198	0.06231	15	0.036145	0.58
		> 500	408601	0.649517	164	0.395181	0.61

Table 5.3: Weight values of landslide causative factors by WoE method

SN	LCF	Class	Class pixels counts	Landslide pixel counts	Landslide pixel outside class	Pixels of stable area in a class	Pixels of stable area outside class	W+	W-	Weight of contrast
1	AAR (mm)	1395.48 - 1513.38	25659	17	398	25642	603021	0.004299	-0.00018	0.004482
		1513.38 - 2017.84	282041	179	236	281862	346801	-0.03871	0.030397	-0.06911
		2017.34 - 2522.30	321378	219	196	321159	307504	0.032452	-0.03506	0.067509
2	Geology	Himal Group	74906	115	300	74791	553839	0.845499	-0.19783	1.043326
		Shiprin Khola Formation	192139	137	278	192002	436628	0.077739	-0.0362	0.113936
		Sarung Khola Formation	358962	163	252	358799	269831	-0.37375	0.346898	-0.72065
		Cs	2104	0	415	2104	626526	0	0.003353	-0.00335
		Ulleri Formation	934	0	415	934	627696	0	0.001487	-0.00149
3	Soils Types	CMu	37229	5	410	37224	591406	-1.59225	0.048919	-1.64117
		CMx	484031	284	131	483747	144883	-0.11732	0.314535	-0.43186
		CMe	38813	56	359	38757	589873	0.783305	-0.08132	0.864625
		RGe	27952	50	365	27902	600728	0.998589	-0.08298	1.08157
		CMg	41020	20	395	41000	587630	-0.30258	0.018053	-0.32063
4	Slope (°)	0 - 15	128826	22	393	128804	499823	-1.35199	0.174815	-1.5268
		15 - 30	356339	209	206	356130	272497	-0.1177	0.135508	-0.25321
		30 - 45	136156	174	241	135982	492645	0.661792	-0.29973	0.961525
		45 - 60	7693	10	405	7683	620944	0.678835	-0.01209	0.690929
		> 60	28	0	415	28	628599	0	4.45E-05	-4.5E-05
5	Elevation (m)	379 - 967	85333	68	347	85265	543362	0.189003	-0.03319	0.222195
		967 - 1365	139158	85	330	139073	489554	-0.07709	0.020857	-0.09795
		1365 - 1738	141716	36	379	141680	486947	-0.95479	0.16464	-1.11943
		1738 - 2132	125100	75	340	125025	503602	-0.09577	0.022419	-0.11818
		2132 - 2578	90532	133	282	90399	538228	0.801375	-0.23112	1.032491
		2578 - 3597	47203	18	397	47185	581442	-0.54844	0.033685	-0.58213
6	Curvature	convex (< - 0.05)	303337	222	193	303115	325512	0.103825	-0.10745	0.211274
		Flat (- 0.05 - 0.05)	22945	11	404	22934	605693	-0.31947	0.010301	-0.32977
		Concave (> 0.05)	302760	182	233	302578	326049	-0.09307	0.07925	-0.17232

Table 5.3: Continued

7	Aspects (°)	Flat (-1)	16	0	415	16	628611	0	2.55E-05	-2.5E-05
		North (0 - 22.5; 337.5 - 360)	50929	3	412	50926	577701	0	0.077226	-0.07723
		Northeast (22.5 - 67.5)	51848	31	384	51817	576810	-0.09847	0.008389	-0.10686
		East (67.5 - 112.5)	82487	66	349	82421	546206	0.193074	-0.03266	0.225739
		Southeast (112.5 - 157.5)	96929	84	331	96845	531782	0.272965	-0.05886	0.33182
		South (157.5 - 202.5)	104953	124	291	104829	523798	0.583211	-0.17252	0.755734
		Southwest (202.5 - 247.5)	91899	72	343	91827	536800	0.172019	-0.03264	0.204655
		West (247.5 - 292.5)	79344	32	383	79312	549315	-0.49239	0.054622	-0.54702
		Northwest (292.5 - 337.5)	70637	3	412	70634	557993	0	0.111936	-0.11194
8	NDVI	< 0.15	18	0	415	18	628568	0	2.86E-05	-2.9E-05
		0.15 - 0.30	1746	7	408	1739	626847	1.807794	-0.01424	1.822035
		0.30 - 0.45	13859	46	369	13813	614773	1.618226	-0.09526	1.713488
		0.45 - 0.60	69680	90	325	69590	558996	0.672383	-0.12712	0.799506
		> 0.60	543698	272	143	543426	85160	-0.2769	0.933507	-1.2104
9	TWI	2.426 - 4.881	199249	139	276	199110	429517	0.055876	-0.027	0.082877
		4.881 - 6.146	224200	148	267	224052	404575	0.000594	-0.00033	0.000923
		6.146 - 7.708	122341	72	343	122269	506358	-0.1143	0.025746	-0.14004
		7.708 - 9.791	56408	36	379	56372	572255	-0.03319	0.003211	-0.03641
		9.791 - 13.212	20582	17	398	20565	608062	0	-0.00857	0.008565
		13.212 - 21.469	6262	3	412	6259	622368	0	0.002751	-0.00275
10	Proximity_ roads (m)	< 50	137897	124	291	137773	490896	0.310001	-0.10758	0.417583
		50 - 100	98081	63	352	98018	530651	-0.02669	0.004853	-0.03154
		100 - 150	74850	65	350	74785	553884	0.275096	-0.0437	0.318792
		150 - 200	49206	32	383	49174	579495	-0.0143	0.001204	-0.01551
		200 - 250	49932	29	386	49903	578766	-0.12746	0.010265	-0.13772
		> 250	219118	102	313	219016	409653	-0.34885	0.146219	-0.49506
11	Proximity_ rivers (m)	< 100	54456	91	324	54365	574304	0.930465	-0.15709	1.087554
		100 - 200	43942	52	363	43890	584779	0.584884	-0.0615	0.646388
		200 - 300	44966	59	356	44907	583762	0.68827	-0.07924	0.767506
		300 - 400	37921	34	381	37887	590782	0.307079	-0.02332	0.3304
		400 - 500	39198	15	400	39183	589486	-0.54487	0.02754	-0.57241
		> 500	408601	164	251	408437	220232	-0.49714	0.546098	-1.04324

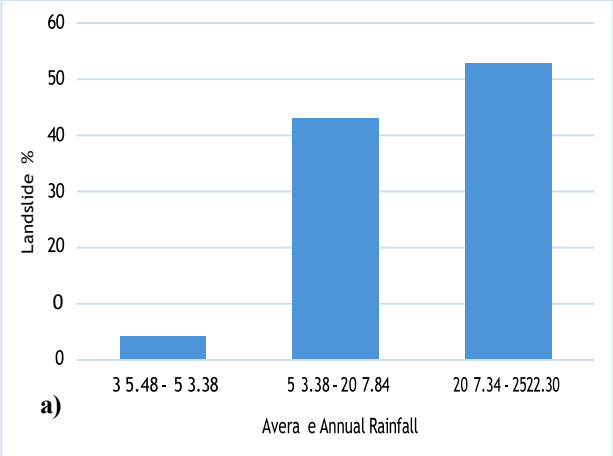
60
50
40
30
20
0
0
Landslide %
3 5.48 - 5 3.38
5 3.38 - 20 7.84
20 7.34 - 2522.30
a)
Avera e Annual Rainfall

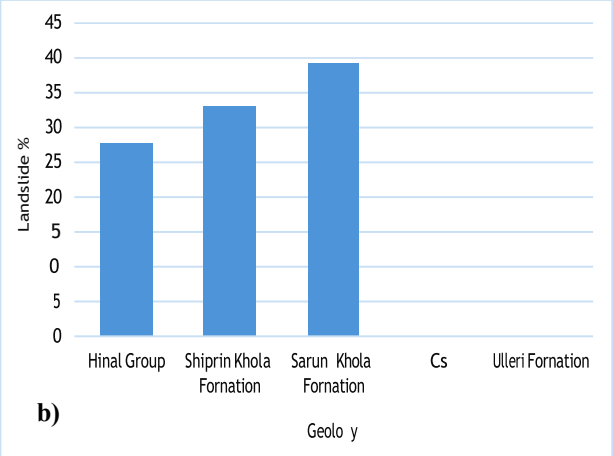
45
40
35
30
25
20
5
0
5
0
Landslide %
Hinal Group
Shiprin Khola Formation
Sarun Khola Formation
Cs
Ulleri Fornation
b)
Geolo y

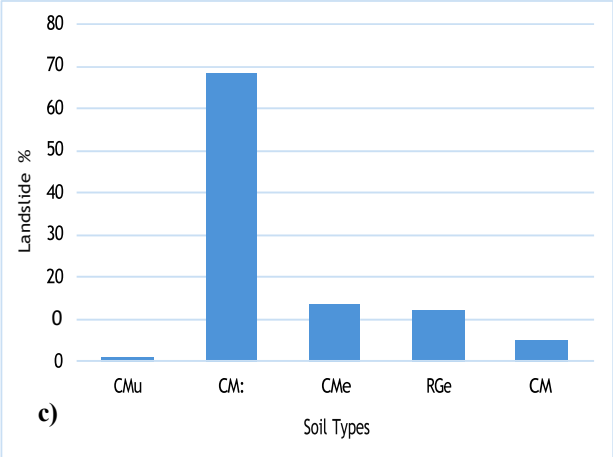
80
70
60
50
40
30
20
0
0
Landslide %
CMu
CM:
CMe
RGe
CM
c)
Soil Types

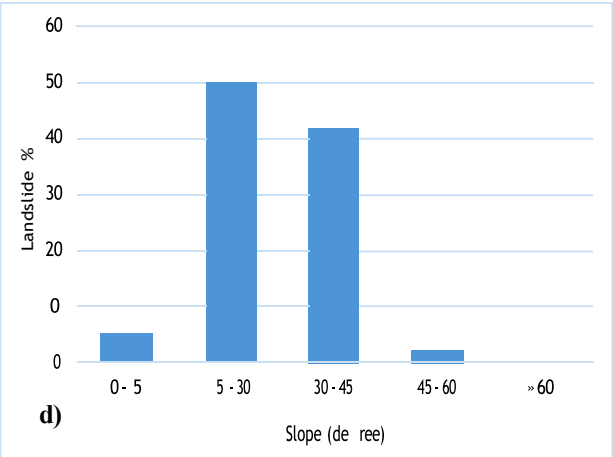
60
50
40
30
20
0
0
Landslide %
0 - 5
5 - 30
30 - 45
45 - 60
» 60
d)
Slope (de ree)

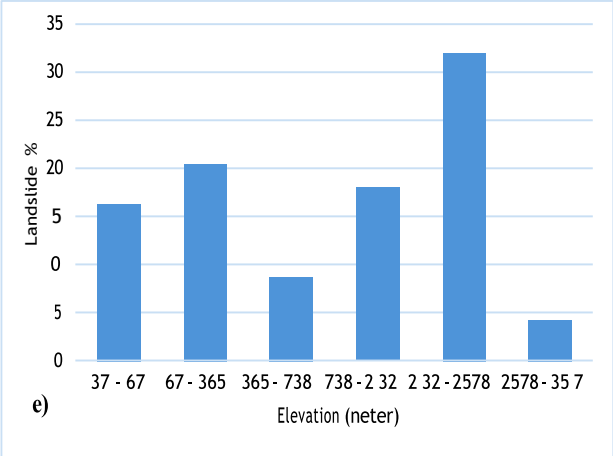
35
30
25
20
5
0
5
0
Landslide %
37 - 67
67 - 365
365 - 738
738 - 2 32
2 32 - 2578
2578 - 35 7
e)
Elevation (neter)

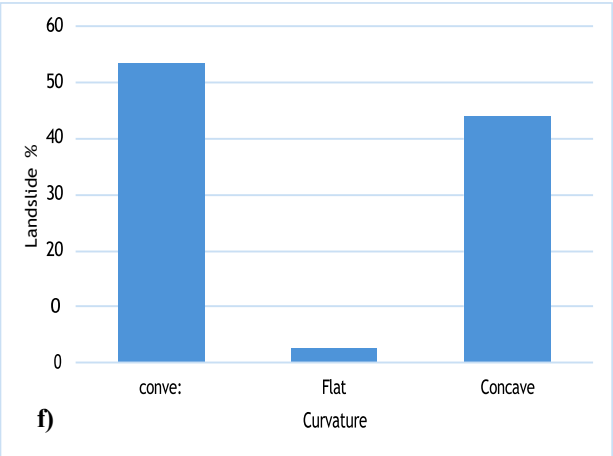
60
50
40
30
20
0
0
Landslide %
conve:
Flat
Concave
f)
Curvature

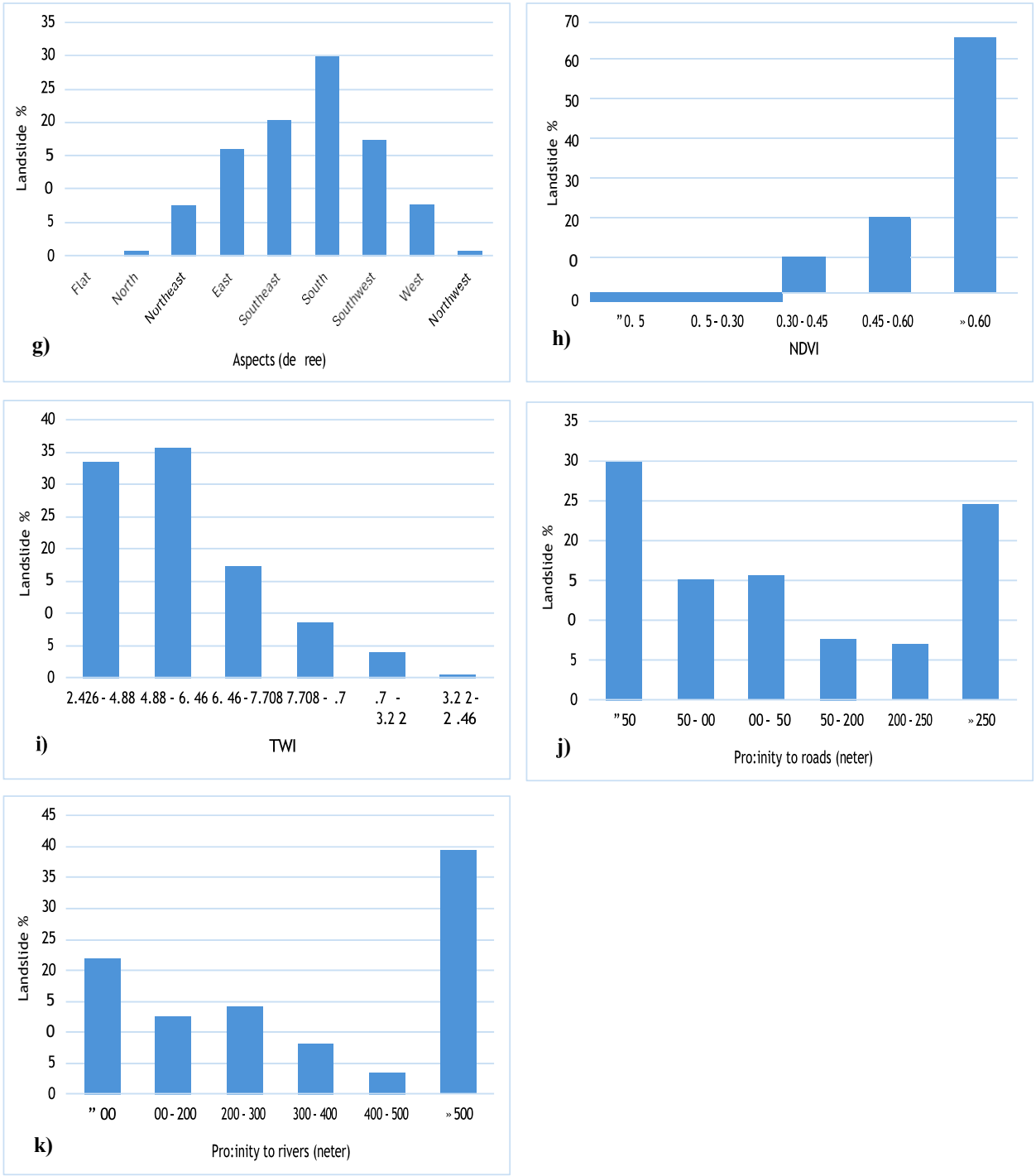

Figure 5.8: Relationship of landslide occurrence with causative factors. (a) AAR (b) Geology (c) Soil types (d) Slope (e) Elevation (f) Curvature (g) Aspects (h) NDVI (i) TWI (j) Road Proximity (k) River Proximity

Table 5.4: PR value of various causative factors

SN	LCF	Prediction Rate (PR)
1	Annual_Rainfall	1
2	Geology	24.7
3	Soil types	16.22
4	Slope (°)	16.91
5	Elevation (m)	12.83
6	Curvature	6.04
7	Aspects (°)	10.87
8	NDVI	19.13
9	TWI	3.83
10	Proximity_roads (m)	4.52
11	Proximity_rivers (m)	9.61

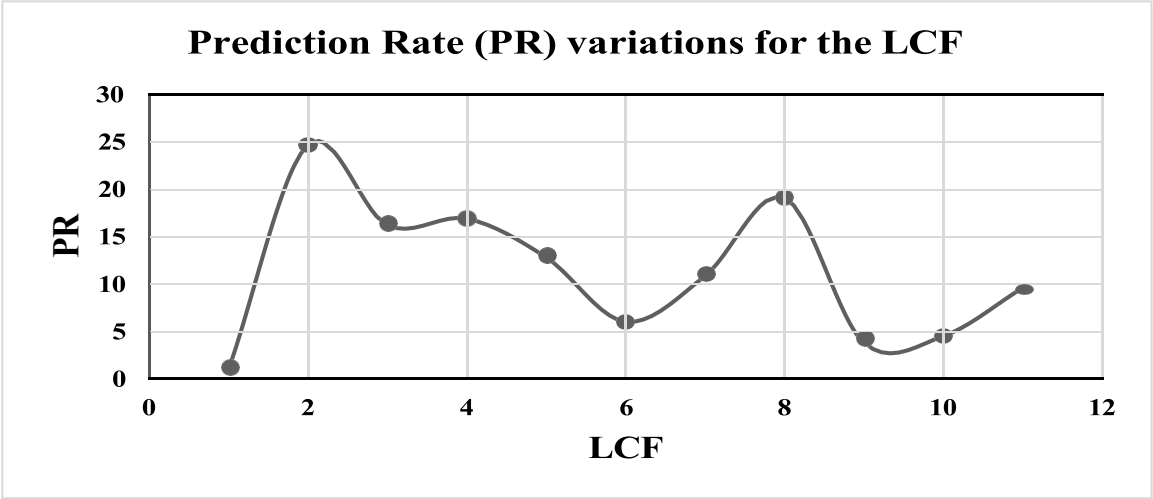

Figure 5.9: PR variations for the LCF

Prediction Rate (PR) analysis further supports these findings: geology (PR = 24.7), NDVI (PR = 19.13), slope (PR = 16.91), and soil types (PR = 5.69) emerge as the strongest predictors of landslide occurrence.

Across all conditioning factors, slope angle (45°-60°), NDVI (0.15–0.30), and river proximity exhibit the highest Frequency Ratios, marking them as the dominant drivers of landslide occurrence in the basin. Geological units (Himal Group, RGe soils) and hydrological triggers (high rainfall) further compound susceptibility, while proximity to rivers and roads introduces both natural and anthropogenic stressors. Together, these findings demonstrate that landslides result from an interplay of extreme topography, weak lithology, monsoonal forcing, and land-use disturbance, with vegetation cover and river corridors acting as the most statistically significant discriminators of hazard-prone terrain.

5.5 Discussion

The landslide susceptibility analysis in the Mai Khola watershed highlights the complex interplay of topographic, geological, hydrological, and anthropogenic factors influencing slope instability, consistent with findings from previous Himalayan studies.

The strong correlation between **slope angle** and landslide occurrence in this study, with the highest susceptibility in the 30°–60° range, mirrors observations in other Himalayan watersheds where moderate to steep slopes are more prone to failure (Dahal & Hasegawa, 2008; Bhandary et al., 2019). Slopes above 60° exhibited minimal landslide occurrence, possibly due to limited soil accumulation or natural slope cleansing, aligning with Aleotti (2004) who noted similar patterns in steep Himalayan terrain.

Aspect was also a significant control; south-facing slopes showed higher landslide probability, likely due to greater exposure to monsoonal rainfall and increased solar radiation that accelerates weathering and reduces soil cohesion (Dahal et al., 2020). This corresponds with regional studies that report similar aspect-related susceptibility in the Himalayas (Chauhan et al., 2020). In contrast, northwest-facing slopes showed very low susceptibility, probably benefiting from reduced rainfall and better drying conditions, which supports findings by Dahal et al. (2020) in nearby Himalayan valleys.

The geological influence observed here, especially the high landslide susceptibility of the **Himal Group formations** (phyllites, slates, and schists), is consistent with Khanal et al. (2022) and Upreti & Dhital (2018), who documented the rapid weathering and clay-rich soil formation from these rocks, making slopes prone to shallow and deep-seated landslides. Conversely, the relatively stable

Sarung Khola formation showed lower susceptibility, reflecting its coarser, more erosion-resistant sediments.

Hydrologically, the proximity to streams (<100 m) being strongly associated with landslides agrees with Sidle & Ochiai (2006) and Rimal et al. (2017), who emphasized toe erosion and water saturation as critical drivers of slope failure in steep Himalayan catchments. Similarly, roads near slopes increased susceptibility, highlighting the negative impacts of infrastructure development through slope cutting and drainage disruption, as reported by Kim et al. (2017).

Vegetation's protective role was clear: areas with low to moderate NDVI (0.15–0.30) had the highest landslide risk, corroborating the stabilizing effect of root networks found in other Himalayan studies (Vrieling et al., 2014; Shrestha et al., 2019). This emphasizes the need for vegetation conservation in landslide-prone zones.

Overall, this study's findings reinforce that landslide occurrences in the Mai Khola watershed are not random but driven by the convergence of multiple high-risk factors, consistent with broader Himalayan research. These insights provide a robust foundation for targeted risk management and sustainable land-use planning in the region.

Chapter 6 : Conclusions

6.1 Conclusions

This study successfully executed a GIS-based landslide susceptibility zonation (LSZ) of the Maikhola Watershed in Ilam District, Nepal, employing two robust bivariate statistical models: Frequency Ratio (FR) and Weight of Evidence (WoE). The primary objective was to generate scientifically reliable hazard zonation maps to serve as critical tools for disaster risk reduction and informed land-use planning in this landslide-prone region and sediment control on the downstream of caused by local road construction.

The research commenced with the compilation of a comprehensive, multi-temporal landslide inventory comprising 300 events, which served as the foundational dataset for model training and validation. Eleven pertinent landslide conditioning factors (LCFs) encompassing topographic, geological, hydrological, and anthropogenic domains were systematically processed within a GIS environment. The application of the FR and WoE models yielded continuous Landslide Susceptibility Index (LSI) values, which were subsequently classified into five distinct hazard zones: Very Low, Low, Moderate, High, and Very High.

The key findings and conclusions of this study are summarized as follows:

1. **High Model Performance and Validation:** Both statistical models demonstrated strong predictive capability. The FR model achieved a very good accuracy with an AUC of 0.854, while the WoE model performed excellently with a superior AUC of 0.866. This high validation accuracy confirms the reliability of the generated susceptibility maps and the appropriateness of the selected methodology and causative factors for the study area.
2. **Spatial Pattern of Hazard:** The resultant susceptibility maps reveal a coherent and physically meaningful spatial distribution of hazard zones. The High and Very High susceptibility areas are not randomly scattered but are conspicuously concentrated along:
    - **Steep topographic slopes,** particularly those exceeding 45°.
    - **River valleys and drainage corridors,** where fluvial undercutting and soil saturation destabilize slopes.

- **Road networks,** highlighting the significant role of anthropogenic activities like slope cutting and improper drainage in triggering landslides. This pattern aligns perfectly with the known geo-environmental character of the Himalayan mid-hills.

3. **Dominant Landslide Controlling Factors:** The feature importance analysis elucidated the primary drivers of landslide occurrence in the Maikhola Watershed. The most significant factors, in order of predictive power, were identified as:
    - **Geology** and **Slope Angle:** Representing the inherent geological weakness and the primary topographic driver of slope instability.
    - **NDVI**: underscoring the critical role of vegetation in stabilizing slopes. Areas with sparse vegetation (low NDVI) were exceptionally prone.
    - **Annual Rainfall:** Quantifying the primary triggering mechanism, confirming the dominance of monsoon-driven landslide events in the region.
4. **Comparative Model Analysis:** While both models are effective, the WoE model provided a more refined and spatially precise delineation of the most critical zones. The WoE model's Bayesian nature, which accounts for the conditional independence of factors, likely makes it more robust against overestimation compared to the FR model, especially in heterogeneous terrains.

In conclusion, this study has transcended its primary aim by not only producing high-accuracy susceptibility maps but also by providing a quantitative understanding of the factors controlling landslide distribution in the Maikhola Watershed. The final maps constitute a vital decision-support tool for local authorities, planners, and disaster management committees, enabling them to prioritize areas for mitigation efforts, enforce building codes, and guide future development away from high-risk zones, thereby enhancing community resilience.

6.2 Limitations

This study has some limitations due to how it was done and the information that was available.

Inventory Bias and Completeness: The landslide inventory might not be complete. It is possible that smaller landslides were missed, especially if they were hard to reach or were covered by thick plants and trees. Also, this list was made over some period of time; it might not show how often these events actually happen over a longer period due to the unavailability of Google Earth satellite image data.

Data Resolution and Scale: The use of 30 m resolution, while used for a watershed-scale study, limits the detection of critical features that make a slope unstable, like a small spring of water, a rocky outcrop, or a very sharp drop. It might miss the exact spot where a small, dangerous landslide could happen. The geological map scale (1:1,000,000) is highly generalized and cannot capture detailed structural features like joints and small-scale faults, which are critical local controls.

Static Model Assumption: The landslide model is static, meaning it doesn't change. It uses an average idea of yearly rain, but it can't predict what would happen during one single, massive storm or earthquake. These sudden, extreme events can cause many more landslides than the model shows.

Methodological Constraints: Bivariate models like FR and WoE analyze factors that have their own constraints. The assumption that future landslides will occur under conditions similar to past events may not always hold, if the weather pattern changes or if people change how they use the land.

REFERENCES

Abella, E. A. C., & Van Westen, C. J. (2007). Generation of a landslide risk index map for Cuba using spatial multi-criteria evaluation. *Landslides*, *4*(4), 311–325. https://doi.org/10.1007/s10346-007-0087-y

Acharya, T. D. (2018). Regional scale landslide hazard assessment using machine learning methods in Nepal. *Esis for: Doctor in EngineeringAdvisor,, Esis for: Doctor in EngineeringAdvisor*.

Adhikari, B. R., & Gautam, S. (2022). A Review of Policies and Institutions for Landslide Risk Management in Nepal. *Nepal Public Policy Review*, *2*, 93–112. https://doi.org/10.3126/nppr.v2i1.48397

ADPC. (2010). Nepal Hazard Risk Assessment. In *Disaster Risk Assessment and Monitoring*. Government of Nepal, Ministry of Home Affairs.

Amare, S., Langendoen, E., Keesstra, S., van der Ploeg, M., Gelagay, H., Lemma, H., & van der Zee, S. E. A. T. M. (2021). Susceptibility to gully erosion: Applying random forest (RF) and frequency ratio (FR) approaches to a small catchment in Ethiopia. *Water (Switzerland)*, *13*(2). https://doi.org/10.3390/w13020216

Baral, N., Kumar Karna, A., & Gautam, S. (2021a). Landslide Susceptibility Assessment Using Modified Frequency Ratio Model in Kaski District, Nepal. *Nepal (March 1, 2021)*.

Baral, N., Kumar Karna, A., & Gautam, S. (2021b). Landslide Susceptibility Assessment Using Modified Frequency Ratio Model in Kaski District, Nepal. *Nepal (March 1, 2021)*.

Bilham, R. (2019). Himalayan earthquakes: A review of historical seismicity and early 21st century slip potential. *Geological Society Special Publication*, *483*(1), 423–482. https://doi.org/10.1144/SP483.16

BINH, P. T. (2017). *Modeling of Landslide Hazard Assessment Using Geo-Informatics Techniques*. Gujarat Technological University Ahmedabad.

Bobrowsky, P., & Highland, L. (2013). The Landslide Handbook- A Guide to Understanding Landslides: A landmark publication for landslide education and preparedness. *Landslides: Global Risk Preparedness*, 75–84. https://doi.org/10.1007/978-3-642-22087-6_5

Castellanos Abella, E. A., & Van Westen, C. J. (2008). Qualitative landslide susceptibility assessment by multicriteria analysis: A case study from San Antonio del Sur, Guantánamo, Cuba. *Geomorphology*, *94*(3–4), 453–466. https://doi.org/10.1016/j.geomorph.2006.10.038

Cruden, D. M. (1993a). Cruden, DM, Varnes, DJ, 1996, Landslide Types and Processes, Transportation Research Board, US National Academy of Sciences, Special Report, 247: 36-75. *Landslides Eng. Pract*, *24*(December), 20–47.

Cruden, D. M. (1993b). Cruden, DM, Varnes, DJ, 1996, Landslide Types and Processes, Transportation Research Board, US National Academy of Sciences, Special Report, 247: 36-75. *Landslides Eng. Pract*, *24*(December), 20–47.

Dai, F. C., Lee, C. F., & Ngai, Y. Y. (2002a). Landslide risk assessment and management: An overview. *Engineering Geology*, *64*(1), 65–87. https://doi.org/10.1016/S0013-7952(01)00093-X

Dai, F. C., Lee, C. F., & Ngai, Y. Y. (2002b). Landslide risk assessment and management: An overview. *Engineering Geology*, *64*(1), 65–87. https://doi.org/10.1016/S0013-7952(01)00093-X

Devkota, K. C., Regmi, A. D., Pourghasemi, H. R., Yoshida, K., Pradhan, B., Ryu, I. C., Dhital, M. R., & Althuwaynee, O. F. (2013a). Landslide susceptibility mapping using certainty factor, index of entropy and logistic regression models in GIS and their comparison at Mugling-Narayanghat road section in Nepal Himalaya. *Natural Hazards*, *65*(1), 135–165. https://doi.org/10.1007/s11069-012-0347-6

Froude, M. J., & Petley, D. N. (2018a). Global fatal landslide occurrence from 2004 to 2016. *Natural Hazards and Earth System Sciences*, *18*(8), 2161–2181. https://doi.org/10.5194/nhess-18-2161-2018

Froude, M. J., & Petley, D. N. (2018b). Global fatal landslide occurrence from 2004 to 2016. *Natural Hazards and Earth System Sciences*, *18*(8), 2161–2181. https://doi.org/10.5194/nhess-18-2161-2018

Gupta, D. (2022a). *Interpretable Machine Learning Methods for Landslide Analysis*. Massachusetts Institute of Technology.

Gupta, D. (2022b). *Interpretable Machine Learning Methods for Landslide Analysis*. Massachusetts Institute of Technology.

Guzzetti, F., Mondini, A. C., Cardinali, M., Fiorucci, F., Santangelo, M., & Chang, K. T. (2012). Landslide inventory maps: New tools for an old problem. *Earth-Science Reviews*, *112*(1–2), 42–66. https://doi.org/10.1016/j.earscirev.2012.02.001

Guzzetti, F., Reichenbach, P., Cardinali, M., Galli, M., & Ardizzone, F. (2005). Probabilistic landslide hazard assessment at the basin scale. *Geomorphology*, *72*(1–4), 272–299. https://doi.org/10.1016/j.geomorph.2005.06.002

Hasegawa, S., Dahal, R. K., Yamanaka, M., Bhandary, N. P., Yatabe, R., & Inagaki, H. (2009). Causes of large-scale landslides in the Lesser Himalaya of central Nepal. *Environmental Geology*, *57*(6), 1423–1434. https://doi.org/10.1007/s00254-008-1420-z

Herrera, M. H. (2016). *L andslide Detection using Random Forest Classifier*.

Highland, L. M., & Bobrowsky, P. (2008). The landslide Handbook - A guide to understanding landslides. *US Geological Survey Circular*, *1325*, 1–147.

Kalantar, B., Pradhan, B., Amir Naghibi, S., Motevalli, A., & Mansor, S. (2018). Assessment of the effects of training data selection on the landslide susceptibility mapping: a comparison between support vector machine (SVM), logistic regression (LR) and artificial neural networks (ANN). *Geomatics, Natural Hazards and Risk*, *9*(1), 49–69. https://doi.org/10.1080/19475705.2017.1407368

Kavzoglu, T., Sahin, E. K., & Colkesen, I. (2014a). Landslide susceptibility mapping using GIS-based multi-criteria decision analysis, support vector machines, and logistic regression. *Landslides*, *11*(3), 425–439. https://doi.org/10.1007/s10346-013-0391-7

Kavzoglu, T., Sahin, E. K., & Colkesen, I. (2014b). Landslide susceptibility mapping using GIS-based multi-criteria decision analysis, support vector machines, and logistic regression. *Landslides*, *11*(3), 425–439. https://doi.org/10.1007/s10346-013-0391-7

Khatakho, R., Gautam, D., Aryal, K. R., Pandey, V. P., Rupakhety, R., Lamichhane, S., Liu, Y. C., Abdouli, K., Talchabhadel, R., Thapa, B. R., & Adhikari, R. (2021a). Multi-hazard risk assessment of kathmandu valley, Nepal. *Sustainability (Switzerland)*, *13*(10), 5369. https://doi.org/10.3390/su13105369

Khatakho, R., Gautam, D., Aryal, K. R., Pandey, V. P., Rupakhety, R., Lamichhane, S., Liu, Y. C., Abdouli, K., Talchabhadel, R., Thapa, B. R., & Adhikari, R. (2021b). Multi-hazard risk assessment of kathmandu valley, Nepal. *Sustainability (Switzerland)*, *13*(10), 5369. https://doi.org/10.3390/su13105369

Maes, J., Kervyn, M., de Hontheim, A., Dewitte, O., Jacobs, L., Mertens, K., Vanmaercke, M., Vranken, L., & Poesen, J. (2017). Landslide risk reduction measures: A review of practices and challenges for the tropics. *Progress in Physical Geography*, *41*(2), 191–221. https://doi.org/10.1177/0309133316689344

Marjanović, M. (2013a). *Advanced methods for landslide assessment using GIS*. Palacký University Olomouc Olomouc, Czechia.

Marjanović, M. (2013b). *Advanced methods for landslide assessment using GIS*. Palacký University Olomouc Olomouc, Czechia.

Ngo, T. Q., Dam, N. D., Al-Ansari, N., Amiri, M., Phong, T. Van, Prakash, I., Le, H. Van, Nguyen, H. B. T., & Pham, B. T. (2021a). Landslide Susceptibility Mapping Using Single Machine Learning Models: A Case Study from Pithoragarh District, India. *Advances in Civil Engineering*, *2021*. https://doi.org/10.1155/2021/9934732

Ngo, T. Q., Dam, N. D., Al-Ansari, N., Amiri, M., Phong, T. Van, Prakash, I., Le, H. Van, Nguyen, H. B. T., & Pham, B. T. (2021b). Landslide Susceptibility Mapping Using Single Machine Learning Models: A Case Study from Pithoragarh District, India. *Advances in Civil Engineering*, *2021*. https://doi.org/10.1155/2021/9934732

Okamura, M., Bhandary, N. P., Mori, S., Marasini, N., & Hazarika, H. (2015a). Report on a reconnaissance survey of damage in Kathmandu caused by the 2015 Gorkha Nepal earthquake. *Soils and Foundations*, *55*(5), 1015–1029. https://doi.org/10.1016/j.sandf.2015.09.005

Okamura, M., Bhandary, N. P., Mori, S., Marasini, N., & Hazarika, H. (2015b). Report on a reconnaissance survey of damage in Kathmandu caused by the 2015 Gorkha Nepal earthquake. *Soils and Foundations*, *55*(5), 1015–1029. https://doi.org/10.1016/j.sandf.2015.09.005

Pacheco Quevedo, R., Velastegui-Montoya, A., Montalván-Burbano, N., Morante-Carballo, F., Korup, O., & Daleles Rennó, C. (2023). Land use and land cover as a conditioning factor in landslide susceptibility: a literature review. *Landslides*, *20*(5), 967–982. https://doi.org/10.1007/s10346-022-02020-4

Paudyal, N., Khadka, R. B., & Khadka, R. (2013). Agricultural perspectives of climate change induced disasters in Doti, Nepal. *Journal of Agriculture and Environment*, *14*, 149–159. https://doi.org/10.3126/aej.v14i0.19795

Rahman, G., Bacha, A. S., Ul Moazzam, M. F., Rahman, A. U., Mahmood, S., Almohamad, H., Al Dughairi, A. A., Al-Mutiry, M., Alrasheedi, M., & Abdo, H. G. (2022). Assessment of landslide susceptibility, exposure, vulnerability, and risk in shahpur valley, eastern hindu kush. *Frontiers in Earth Science*, *10*(August), 1–23. https://doi.org/10.3389/feart.2022.953627

Rahmati, O., Yousefi, S., Kalantari, Z., Uuemaa, E., Teimurian, T., Keesstra, S., Pham, T. D., & Bui, D. T. (2019a). Multi-hazard exposure mapping using machine learning techniques: A case study from Iran. *Remote Sensing*, *11*(16), 1–20. https://doi.org/10.3390/rs11161943

Rahmati, O., Yousefi, S., Kalantari, Z., Uuemaa, E., Teimurian, T., Keesstra, S., Pham, T. D., & Bui, D. T. (2019b). Multi-hazard exposure mapping using machine learning techniques: A case study from Iran. *Remote Sensing*, *11*(16), 1–20. https://doi.org/10.3390/rs11161943

Saaty, T. L. (1990). How to make a decision: The analytic hierarchy process. *European Journal of Operational Research*, *48*(1), 9–26. https://doi.org/10.1016/0377-2217(90)90057-I

Sarkar, S., & Kanungo, D. (2006). GIS Based landslide susceptibility mapping—a case study in Indian Himalaya. *Proc. Interpraevent Int. …*, *May 2014*, 617–624.

Shano, L., Raghuvanshi, T. K., & Meten, M. (2020). Landslide susceptibility evaluation and hazard zonation techniques – a review. *Geoenvironmental Disasters*, *7*(1). https://doi.org/10.1186/s40677-020-00152-0

Sreelakshmi, S., Vinod Chandra, S. S., & Shaji, E. (2022). Landslide identification using machine learning techniques: Review, motivation, and future prospects. *Earth Science Informatics*, *15*(4), 2063–2090. https://doi.org/10.1007/s12145-022-00889-2

Titti, G., Borgatti, L., Zou, Q., Cui, P., & Pasuto, A. (2021). Landslide susceptibility in the Belt and Road Countries: continental step of a multi-scale approach. *Environmental Earth Sciences*, *80*(18), 1–18. https://doi.org/10.1007/s12665-021-09910-1

Uddin, K., Matin, M. A., & Maharjan, S. (2018). Assessment of land cover change and its impact on changes in soil erosion risk in Nepal. *Sustainability (Switzerland)*, *10*(12). https://doi.org/10.3390/su10124715

Varnes, D. (1978a). Slope Movement Types and Processes. *Special Report*, *176*, 11–33.

Varnes, D. (1978b). Slope Movement Types and Processes. *Special Report*, *176*, 11–33.

Varnes, D. J. (1984a). *Landslide hazard zonation: a review of principles and practice* (Issue 3).

Varnes, D. J. (1984b). *Landslide hazard zonation: a review of principles and practice* (Issue 3).

Wang, H., Zhang, L., Yin, K., Luo, H., & Li, J. (2021). Landslide identification using machine learning. *Geoscience Frontiers*, *12*(1), 351–364. https://doi.org/10.1016/j.gsf.2020.02.012

Ward, P. J., Blauhut, V., Bloemendaal, N., Daniell, E. J., De Ruiter, C. M., Duncan, J. M., Emberson, R., Jenkins, F. S., Kirschbaum, D., Kunz, M., Mohr, S., Muis, S., Riddell, A. G., Schäfer, A., Stanley, T., Veldkamp, I. E. T., & Hessel, W. C. (2020). Review article: Natural hazard risk assessments at the global scale. *Natural Hazards and Earth System Sciences*, *20*(4), 1069–1096. https://doi.org/10.5194/nhess-20-1069-2020

Zhu, A. X., Miao, Y., Liu, J., Bai, S., Zeng, C., Ma, T., & Hong, H. (2019). A similarity-based approach to sampling absence data for landslide susceptibility mapping using data-driven methods. *Catena*, *183*(October 2018), 104188.

APPENDICS

Field Visit and Survey Photographs For Landslide Inventory Collections

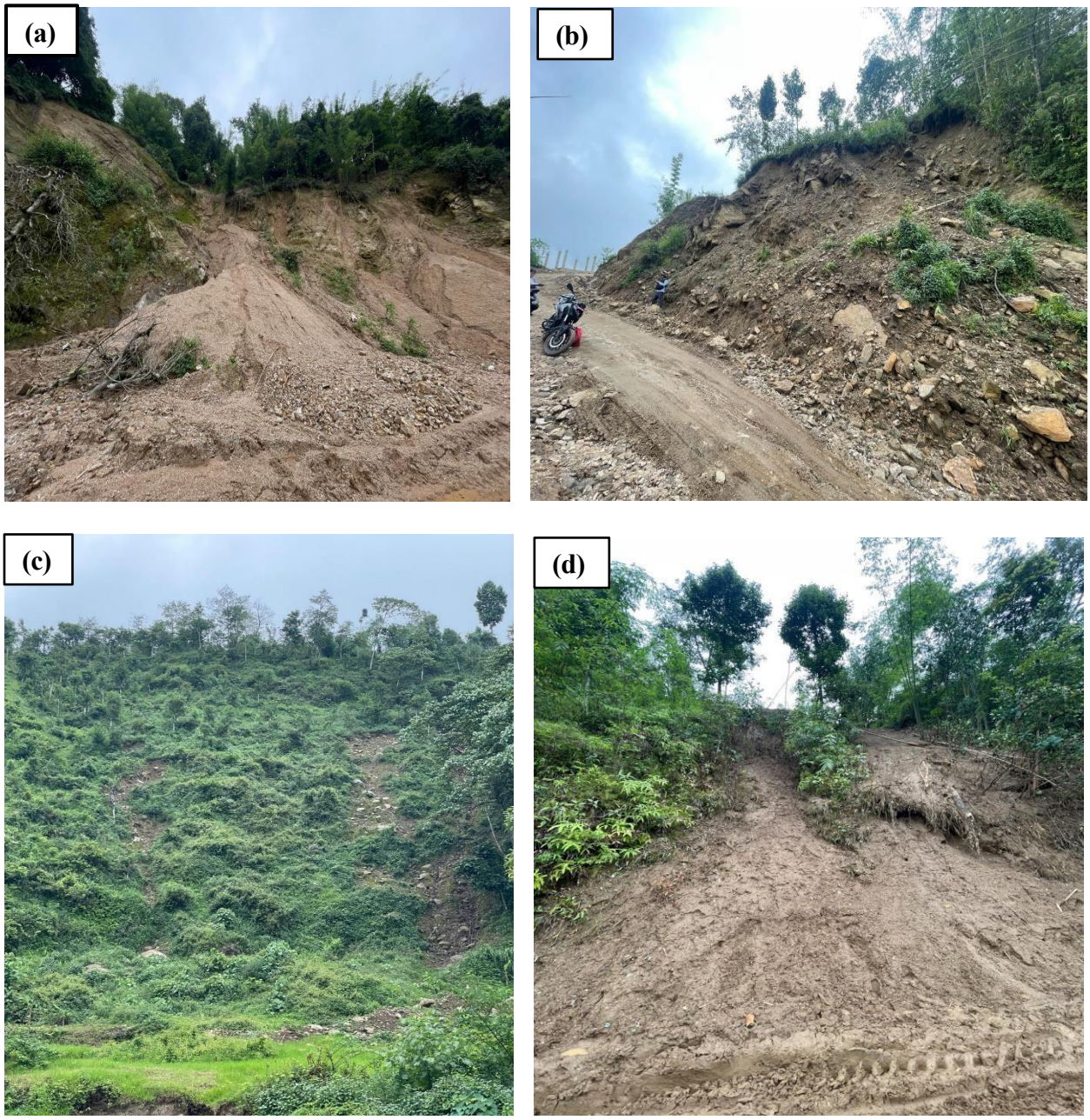

Figure A1: **(a)** Landslide near Mai-Pokhari (26° 59' 57.80N,"87° 55' 41.10"E) **(b)** Landslide at Sulubung(27° 01' 03.10"N,87° 57' 19.20"E) **(c)** Landslide near Maimajhuwa (27° 03' 35.10"N, 87° 56' 46.50"E) **(d)** Landslide near Todke Jharna (27° 02' 28.50"N,87° 56' 56.30"E)

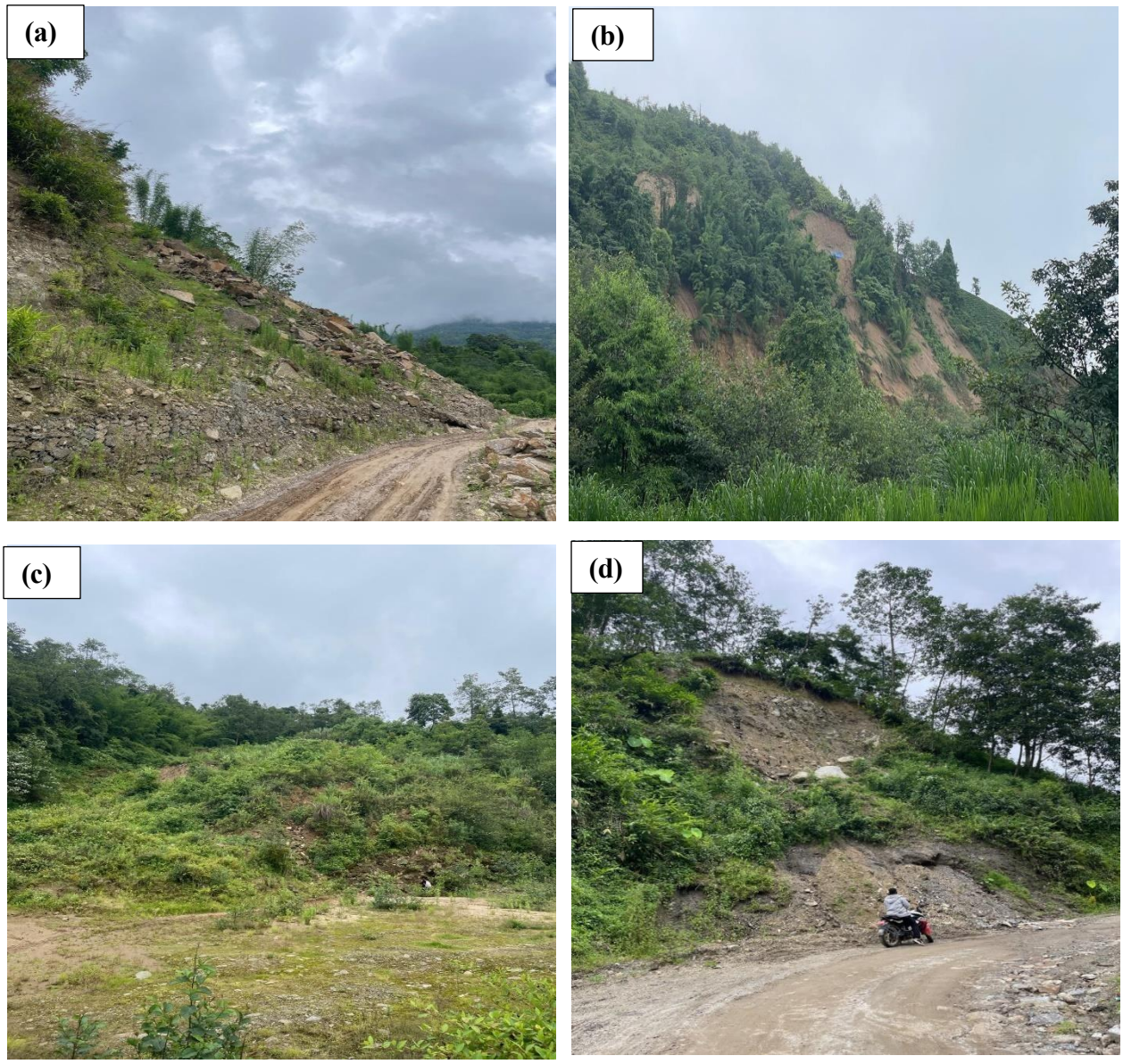

Figure A2: **(a)**Landslide near Subulung(27° 01' 03.10"N,87° 57' 23.90"E) **(b)** Landslide near Mai-Pokhari (26° 59' 57.80N,"87° 55' 41.10"E) **(c)** Landslide at Deurali(27° 01' 02.80"N, 87° 55' 37.00"E) **(d)** Landslide near Mai Valley Hydropower (27° 01' 29.00"N,87° 57' 24.70"E).